Published in final edited form as:

J Cogn Neurosci. 2023 February 01; 35(2): 200–225. doi:10.1162/jocn_a_01945.

Hemispheric Asymmetries of Individual Differences in Functional Connectivity

Diana C. Perez[1], **Ally Dworetsky**[1], **Rodrigo M. Braga**[1], **Mark Beeman**[1], **Caterina Gratton**[1,2]

[1]Northwestern University, Evanston, IL,

[2]Florida State University, Tallahassee

Abstract

Resting-state fMRI studies have revealed that individuals exhibit stable, functionally meaningful divergences in large-scale network organization. The locations with strongest deviations (called network "variants") have a characteristic spatial distribution, with qualitative evidence from prior reports suggesting that this distribution differs across hemispheres. Hemispheric asymmetries can inform us on constraints guiding the development of these idiosyncratic regions. Here, we used data from the Human Connectome Project to systematically investigate hemispheric differences in network variants. Variants were significantly larger in the right hemisphere, particularly along the frontal operculum and medial frontal cortex. Variants in the left hemisphere appeared most commonly around the TPJ. We investigated how variant asymmetries vary by functional network and how they compare with typical network distributions. For some networks, variants seemingly increase group-average network asymmetries (e.g., the group-average language network is slightly bigger in the left hemisphere and variants also appeared more frequently in that hemisphere). For other networks, variants counter the group-average network asymmetries (e.g., the default mode network is slightly bigger in the left hemisphere, but variants were more frequent in the right hemisphere). Intriguingly, left- and right-handers differed in their network variant asymmetries for the cingulo-opercular and frontoparietal networks, suggesting that variant asymmetries are connected to lateralized traits. These findings demonstrate that idiosyncratic aspects of brain organization differ systematically across the hemispheres. We discuss how these asymmetries in brain organization may inform us on developmental constraints of network variants and how they may relate to functions differentially linked to the two hemispheres.

Reprint requests should be sent to Caterina Gratton, Interdepartmental Neuroscience Program, Northwestern University, 320 E. Superior St., Evanston, IL 60611, or via caterina.gratton@northwestern.edu.

Diversity in Citation Practices

Retrospective analysis of the citations in every article published in this journal from 2010 to 2021 reveals a persistent pattern of gender imbalance: Although the proportions of authorship teams (categorized by estimated gender identification of first author/last author) publishing in the *Journal of Cognitive Neuroscience* (*JoCN*) during this period were M(an)/M = .407, W(oman)/M = .32, M/W = .115, and W/W = .159, the comparable proportions for the articles that these authorship teams cited were M/M = .549, W/M = .257, M/W = .109, and W/W = .085 (Postle and Fulvio, *JoCN*, 34:1, pp. 1–3). Consequently, *JoCN* encourages all authors to consider gender balance explicitly when selecting which articles to cite and gives them the opportunity to report their article's gender citation balance. The authors of this article report its proportions of citations by gender category to be as follows: M/M = .470, W/M = .240, M/W = .120, and W/W = .170.

INTRODUCTION

Resting-state fMRI (rs-fMRI) has become a powerful tool for studying the underlying functional architecture of the brain by examining correlated intrinsic activity between brain regions (Biswal, Yetkin, Haughton, & Hyde, 1995; for reviews, see Power, Schlaggar, & Petersen, 2015; Buckner, Krienen, & Yeo, 2013). This approach has resulted in a robust description of functional networks that are linked to cognitive and sensorimotor processes (Doucet et al., 2011; Power et al., 2011; Yeo et al., 2011). The majority of research on this topic has used the traditional approach of grouping data together from many participants. However, there is individual variability in functional network organization, particularly in association cortex (Finn et al., 2015; Miranda-Dominguez et al., 2014; Mueller et al., 2013). Thus, unique features at the individual level are blurred as a result of averaging across brains with varying network topography.

Recent efforts to map network architectures at the individual level have used precision fMRI, an approach in which experimenters collect extended amounts of rs-fMRI data across multiple sessions for each participant to obtain highly reliable individualized measurements (Greene et al., 2020; Braga & Buckner, 2017; Gordon, Laumann, Gilmore, et al., 2017; Laumann et al., 2015). Although precision fMRI studies suggest that functional networks follow roughly the same organizational principles across participants, each person also exhibits idiosyncratic features: Localized regions where an individual's functional connectivity pattern differs markedly from the group average (i.e., the region shows a pattern of connectivity that is more correlated with a different network than what would typically be found at that location; Seitzman et al., 2019; Gordon, Laumann, Gilmore, et al., 2017; Laumann et al., 2015). We refer to these regions of individual difference as network variants (henceforth also referred to as variants). Network variants can arise for two reasons: either due to relatively local shifts in the borders between networks ("border variants") or due to more dramatic changes in network organization far from the typically associated network ("ectopic intrusions"; Dworetsky, Seitzman, Adeyemo, Neta, et al., 2021). Although variants (of both types) are widespread, individuals differ in the precise location, size, network characteristics, and forms of network variants they exhibit (Dworetsky, Seitzman, Adeyemo, Smith, et al., 2021; Seitzman et al., 2019). Initial studies demonstrate that individual differences in brain network organization relate to individual differences in cognition measured outside the scanner (Kong et al., 2019; Seitzman et al., 2019; Bijsterbosch et al., 2018) as well as differences in task evoked responses during MRI (Seitzman et al., 2019).

Network variants have been shown to be stable over time and to exhibit a characteristic spatial distribution—they are most commonly observed in frontal and temporo-parietal cortex in regions overlapping higher-order cognitive networks in the group average (Seitzman et al., 2019). Additionally, network variants are often associated with higher-level attention, default, and language networks and rarely associated with networks involved in sensorimotor processes. Intriguingly, by visual examination, these individual differences appear to be relatively lateralized, with seemingly more variants appearing in the right hemisphere (see Figure 3A in Seitzman et al., 2019). Factors including evolutionary (Buckner & Krienen, 2013), genetic (Anderson et al., 2021), and experiential variables

(Newbold et al., 2021) have been proposed to guide the organization of closely juxtaposed networks as they fractionate and specialize in the cortex (DiNicola & Buckner, 2021). However, the constraints that influence how and where individual differences in these networks occur are currently largely unknown.

Examining hemispheric asymmetries in network variants may inform how individual differences in functional brain organization arise. Although there is a large degree of homology between the two hemispheres, several asymmetries have been reported in the human brain, ranging from functional to anatomical and cytoarchitectonic in nature (see Toga & Thompson, 2003, for a review). Macrostructural asymmetries are observed in a number of locations, including the trajectory of the Sylvian fissure (Hou et al., 2019), the volume of the temporal plane (Steinmetz, 1996; Geschwind & Levitsky, 1968), and in frontal and occipital petalia (Kong et al., 2018, 2021). In addition, the two hemispheres have been differentially tied to specific functions. Perhaps the most notable examples for asymmetric function are language and visuospatial attention. Although the right hemisphere makes important contributions to language processing (Federmeier, Wlotko, & Meyer, 2008; Lindell, 2006; Jung-Beeman, 2005), most individuals exhibit left-hemispheric dominance for core language function (Stippich et al., 2003; Breier, Simos, Zouridakis, & Papanicolaou, 2000), especially language production (Cai, Van der Haegen, & Brysbaert, 2013; Lidzba, Schwilling, Grodd, Krägeloh-Mann, & Wilke, 2011). In contrast, the majority of the population exhibits right-hemisphere bias for visuospatial processing (Cai et al., 2013; Weintraub & Mesulam, 1987). Asymmetries can also be present in behavioral traits like handedness, auditory perception, and motor preferences (Toga & Thompson, 2003). Functional brain networks also show hemispheric differences in group averages (Wang, Buckner, & Liu, 2014; Gotts et al., 2013). This is especially true in the default mode network (DMN), which shows a left-hemispheric specialization (strong within-hemispheric interactions); the ventral and dorsal attention networks, which show right-hemispheric specialization; and the frontoparietal network, which shows specialization in the two hemispheres but couples with different networks in each hemisphere (Wang et al., 2014). The language network is often hard to detect in group averages because of the strong variation across people (Braga, DiNicola, Becker, & Buckner, 2020; Fedorenko, Duncan, & Kanwisher, 2012), but individual data suggest that it is relatively left-lateralized.

These previous investigations show that hemispheric asymmetries exist at every level of brain organization. Here, we ask how individual differences in network organization vary across the two hemispheres by studying asymmetries in the properties of network variants. Such asymmetries can help our understanding of how individual differences arise and may elucidate important aspects of the relationship between brain organization and cognitive function.

In this project, we first examine hemisphere-wide asymmetries in the extent and size of idiosyncratic variant regions in a large group of young adult participants from the Human Connectome Project (HCP). These asymmetries in the general features of variants would suggest differences in the overall developmental constraints of the two hemispheres. For example, a rightward lateralization in the frequency of variants would indicate a more variable architecture of the right hemisphere compared with the left hemisphere across

individuals. Speculatively, this may indicate that the right hemisphere is less constrained by developmental programs and more malleable to experience-dependent reshaping. Next, we focus on specific locations and networks exhibiting hemispheric asymmetries and study how these asymmetries in network variants relate to group-average network asymmetries. Lastly, we investigate a potential link between individual differences in functional connectivity and behavior by looking at the relationship between network variant asymmetries and handedness.

METHODS

Data Sets and Overview

Two independent and publicly available data sets were used for these analyses: The HCP (Van Essen, Ugurbil, et al., 2012) and the Midnight Scan Club (MSC; Gordon, Laumann, Gilmore, et al., 2017). These data sets were used because of their relatively high amounts of low-motion data per participant, which allows individual-specific measures of functional networks to reach high reliability levels. Specifically, network variant measurements of the cortex can reach high reliability (test–retest $r > .8$) with about 45 min of good quality data (Kraus et al., 2021; Laumann et al., 2015).

Our primary analyses were based on a subsample ($n = 384$) of unrelated participants with >45 min of low-motion data from the HCP data set. The HCP 1200 subject release includes 1 hr of resting-state data collected across two sessions for 1018 participants (546 women) between the ages of 22 and 35 years, including data from twins and nontwin siblings (for more details on the demographic breakdown of this sample, the reader is referred to Van Essen et al., 2013). Exclusion criteria for our inclusion of participants from the HCP 1200 subject release included removing participants who did not complete the study, and participants who did not have at least 45 min of high-quality resting-state data after motion censoring (given the reliability of network variants measures cited in the previous paragraph). This resulted in a subsample of 752 participants (423 women; see Seitzman et al., 2019, for more details). If more than one member of a given set of siblings met the previous criteria, the participant with the most data was selected, and their sibling(s) were excluded from most analyses, resulting in the subsample of 384 unrelated participants (210 women). Note that, to increase the number of left-handed individuals, for the left- versus right-hander comparisons, we used the full subsample of 752 participants from the HCP 1200 release, including related individuals. For the handedness group comparisons, participants were categorized into three groups based on their Edinburgh Handedness Inventory scores (Oldfield, 1971), resulting in 40 left-handers (scores between −100 and −41), 670 right-handers (scores between 41 and 100), and 42 ambidexters (scores between −40 and 40).

The MSC was used as a replication data set to confirm the findings of the HCP in a highly sampled precision-fMRI data set. The MSC includes 5 hr of resting-state BOLD data from 10 unrelated participants collected across 10 sessions. Because of high motion and drowsiness, one participant was excluded from analyses (Gordon, Laumann, Gilmore, et al., 2017; Laumann et al., 2015). Thus, data from nine participants (four women, ages

24–34 years, all right-handers) were used to replicate comparisons of spatial distribution of variants.

An additional data set of 120 neurotypical young adults, the WashU 120 data set (60 women, mean age = 24.7 ± 2.4 years; Power, Schlaggar, Lessov-Schlaggar, & Petersen, 2013), was used as the group average from which canonical network templates were derived and to which individual-specific connectivity maps were compared in order to define network variants.

MRI Acquisition Parameters

The HCP data set was collected on a Siemens 3 T Skyra with a 32-channel head coil. T1-weighted (256 sagittal slices, repetition time [TR] = 2400 msec, echo time [TE] = 2.14 msec, 3D MPRAGE sequence) and T2-weighted (256 sagittal slices, TR = 3200 msec, TE = 565 msec, Siemens SPACE sequence) images were collected for each participant using isotropic 0.7-mm voxels (Glasser et al., 2013). High-resolution eyes-open rs-fMRI data were collected using 2-mm isotropic voxels (72 sagittal slices, TR = 720 msec, TE = 33 msec, multiband accelerated pulse sequence with multiband factor = 8; Glasser et al., 2013, 2016). See Glasser et al. (2013, 2016) for additional detailed information on acquisition in the HCP data set.

The MSC data set was collected on a Siemens 3 T Trio with a 12-channel head coil. The data set includes several types of structural data, including four high-resolution T1w images (0.8 mm isotropic voxels, 224 sagittal slices, TE = 3.74 msec, TR = 2400 msec) and four high-resolution T2w images (0.8 mm isotropic voxels, 224 sagittal slices, TE = 479 msec, TR = 3200 msec). Eyes-open rs-fMRI data were collected using a gradient-echo EPI sequence with 4-mm isotropic voxels (36 slices, TE = 27 msec, TR = 2200 msec; Gordon, Laumann, Gilmore, et al., 2017).

The WashU 120 data set was collected on a Siemens 3 T Trio with a 12-channel coil and includes a high-resolution T1-weighted image (176 slices, isotropic 1-mm voxels, TE = 3.06 msec, TR = 2400 msec) and eyes-open resting-state BOLD data (TR = 2500 msec, TE = 27 msec, gradient-echo EPI sequence, 4-mm isotropic voxels; Power et al., 2011).

Preprocessing and Functional Connectivity Processing of Functional Data

Data were preprocessed identically as in Seitzman et al. (2019). Briefly, HCP volumetric resting-state time series from each participant were preprocessed as recommended by the minimal preprocessing pipelines (Glasser et al., 2013). Then, the data underwent field map distortion correction, mode-1000 normalization, motion correction via a rigid body transformation within each run, affine registration of BOLD images to a T1-weighted image, and affine alignment into Montreal Neurological Institute (MNI) space. The MSC data set was preprocessed similarly with the following exceptions: these data also underwent slice timing correction, and the T1-weighted image was mapped onto Talaraich rather than MNI space.

Resting-state data were further denoised using regression of white matter, cerebrospinal fluid, the global signal, six rigid-body parameters, and their derivatives and expansion

terms (Friston, Williams, Howard, Frackowiak, & Turner, 1996). High-motion frames were identified using frame-by-frame displacement and censored to remove bias in functional connectivity (Power, Barnes, Snyder, Schlaggar, & Petersen, 2012). Frames with FD > 0.2 for MSC data (Gordon, Laumann, Gilmore, et al., 2017) and filtered FD > 0.1 for the HCP data (Fair et al., 2020) were flagged as being contaminated by motion and removed from analyses. Note that for two MSC participants (MSC03 and MSC10), the filtered FD (motion parameters low-pass filtered <0.1 Hz) measure was also used to identify to-be-censored frames to address respiratory-related artifacts in their FD parameter (Gratton et al., 2020; Gordon, Laumann, Gilmore, et al., 2017).

For both data sets, the first five frames of each functional run were dropped, the frames that were flagged as motion-contaminated were removed and interpolated using a power spectral matched interpolation (Power et al., 2014), and a temporal bandpass filter was applied from 0.009 to 0.08 Hz. Volumetric BOLD data were then mapped to each participant's midthickness left- and right-hemisphere cortical surfaces generated by FreeSurfer from the atlas-registered T1 (Dale, Fischl, & Sereno, 1999). The native surfaces were then aligned to the fsaverage surface in 32 k fs_LR space, and the two hemispheres were registered to each other using a landmark-based algorithm (Anticevic et al., 2012), such that they would be in geographic correspondence with each other to allow for point-to-point comparisons between each individual and across hemispheres (Glasser et al., 2013). Lastly, surface resting-state time series were spatially smoothed with a geodesic smoothing kernel (σ = 2.55, FWHM = 6 mm). Functional connectivity was then calculated via temporal correlation between each vertex (a point on the cortical surface) time series with every other vertex time series.

Mapping Locations of Individual Differences in Brain Networks

Locations of individual differences in functional network organization were identified using the "network variant" method as in Seitzman et al. (2019). This method was chosen because of its ability to reliably identify regions of strong deviation in individual participants, as opposed to regions that may differ only slightly in functional connectivity patterns. In addition to the results of the network variant method being robust, the network assignments of regions identified as variants have previously been validated using task-evoked activations (i.e., network variants show task-evoked activation in concordance with their assigned networks, and not their spatial location). Figure 1 shows a schematic representation of the full variant identification and functional network assignment procedure.

To begin, a cortical location-to-location (vertex-to-vertex) functional connectivity map was created for each participant based on their BOLD time series, concatenated across runs. Individual-to-group similarity maps were then obtained for each participant by comparing a given individual's connectivity pattern at each vertex to the group average (WashU 120) connectivity pattern at that vertex using spatial correlation. Each participant's similarity map was then thresholded to the lowest decile to identify the 10% of vertices that were most different between the individual and the group average. These vertices with the lowest correlation values were then binarized, and small clusters (<50 vertices) were removed. Susceptibility areas (primarily along the inferior temporal cortex) with mean BOLD signal

under 750 in the group average were set to 0 and excluded from analyses for all individual-specific connectivity maps because of poor signal quality.

To account for nearby, but distinct, network variant regions, these initial network variants were further refined into separable units as in Dworetsky, Seitzman, Adeyemo, Smith, et al. (2021). This procedure takes into account the homogeneity of functional connectivity within a contiguous region, as well as the proportion of the variants' territory that was dominated by a single network. Homogeneity was assessed using PCA of a variant's vertices' seed maps and then calculating the variance explained by the first principal component of the variant (Dworetsky, Seitzman, Adeyemo, Smith, et al., 2021; Gordon et al., 2016). Network dominance was assessed via a vertex-wise template-matching technique that assigned each vertex to the canonical network that was most similar to the vertex's seed map. This similarity was calculated based on the Dice coefficient between the vertex's seed map and each canonical network template, each binarized to the highest 5% of correlations (see Dworetsky, Seitzman, Adeyemo, Smith, et al., 2021). Variants that did not meet the threshold of 66.7% homogeneity and 75% network dominance in the individual network map were split along the network boundaries of a vertex-wise network map, producing the final analyzed network variants. These parameters for homogeneity and network dominance were set based on a pilot data set (the MSC) for which manual ratings were used to flag variant clusters that appeared to be composed of multiple heterogeneous subunits. The parameters used in the refinement process for the larger HCP subsample were the values that were better able to identify such clusters in the pilot data set. Any resulting clusters after the refinement process that were smaller than 30 contiguous vertices were removed because of their small size. Previous analyses have shown that these parameters can identify large clusters that may consist of separate but adjacent network variants (Dworetsky, Seitzman, Adeyemo, Smith, et al., 2021). In addition, some supplemental analyses were conducted with prevariants before this variant refinement procedure (Appendix A).

By definition, network variants are associated with different network patterns than what would normally be found at that location. To assess which large-scale network a variant was associated with, the resulting variants were matched to the best-fitting functional network using network templates from 14 canonical networks: DMN, visual network, frontoparietal network, dorsal attention network, language network, salience network, cingulo-opercular network, somatomotor dorsal and lateral networks, auditory network, temporal pole (T-pole) network, medial-temporal lobe (MTL) network, parietal memory network (PMN), and parietal occipital network (PON). Templates (or average connectivity maps) for each network were generated using data from the WashU 120 data set and binarized by thresholding the top 5% of correlations (Seitzman et al., 2019; Gordon, Laumann, Gilmore, et al., 2017). For each network variant, the average seed map for all vertices within the variant was computed and also binarized to the top 5% of correlations. This binarized variant seed map was then compared in similarity to each of the binarized network template connectivity patterns via Dice coefficient (as in Dworetsky, Seitzman, Adeyemo, Neta, et al., 2021). The variant was then assigned to the network to which it was most similar. Network variants were removed if they did not match to any functional network (Dice = 0) or if more than 50% of their territory overlapped with the territory of its assigned network in the group average. Note that, although here we use the label "language network" to refer to the

network located on the superior temporal gyrus and a portion of the inferior frontal gyrus, this network has also been referred to as the "ventral attention network" in previous reports. However, recent reports suggest that this network is more accurately described as a language network because of its correspondence with the expected distribution of language regions (Lipkin et al., 2022; Braga et al., 2020).

General Size and Number of Network Variants across Hemispheres

The left and right hemispheres exhibit marked asymmetries at every scale of organization; thus, we asked if the properties of individual differences observed in functional connectivity patterns also vary across the two hemispheres. We first examined whether general properties of size and number of variants, and the proportion of each hemisphere labeled as variants. To this end, we compared the total number of network variants, average variant size, and total surface area of variant territory. Network variant size was calculated by converting vertices belonging to each network variant to surface area using the *wb_command* function *-surface-vertex-areas* on the Conte69 group-average midthickness cortical surface (Glasser & Van Essen, 2011). These were then compared between the left and right hemispheres. We also calculated a "magnitude" of asymmetry defined as the difference in the measurements of the two hemispheres divided by the greater value. This resulted in a percentage that indicates how much greater one hemisphere was compared with the other.

Because the values that we measure in this study are likely to exhibit a nonnormal distribution, we used a non-parametric approach to test the significance of the observed differences. Permutation testing was used to test our hypothesis that the properties of variants differ across the two hemispheres by comparing the true difference values to a null distribution created by randomizing the hemisphere labels. Under the null hypothesis, the hemisphere labels would be exchangeable because they do not differ significantly. Thus, to obtain a null distribution of difference values, left- and right-hemisphere labels were permuted by participant by randomly selecting 50% of the participants from the sample and switching the left- and right-hemisphere labels across 1000 permutations. For each permutation, we obtained the difference in the number of variants between the pseudo-left and pseudo-right hemispheres and averaged the differences across participants' permuted hemispheres. We repeated this procedure 1000 times to create the null distribution against which the true difference score was compared. The significance threshold was set at $p < .025$ at either end of the distribution for two-tailed tests. This same test was conducted to test the significance of the difference in average network variant size and overall variant territory. We used false discovery rate (FDR) correction for multiple comparisons across three tests: number of variant regions, overall variant territory, and average variant size.

Spatial Distribution of Variants across Hemispheres

Because some large-scale networks are associated with relatively lateralized functions, we hypothesized that network variants might exhibit different spatial distributions across the hemispheres. We first conducted an omnibus test of the similarity in variant distributions between the left and right hemispheres. Variant maps were overlapped across participants to quantify the frequency of variants at each vertex. The resulting overlap maps contained a value at each vertex for the proportion of participants who have a variant at that location.

The variant frequency maps of the left and right hemispheres were then compared with each other by aligning each homotopic pair and then using spatial correlation to assess the overall (true) similarity of their spatial distribution of variants. Given that the two hemispheres were registered to each other, we define the homotopic pair of a given vertex as the vertex with the same index in the contralateral hemisphere. The significance of the similarity across the two hemisphere was assessed using a permutation approach, where the true similarity was compared with a null distribution of correlation values obtained by randomly switching the hemisphere labels. Under the null hypothesis that the two hemispheres do not differ significantly, we would obtain equivalent similarity values from comparisons of overlap maps from shuffled hemisphere labels as from comparisons of the true overlap between the two hemispheres. Our hypothesis was that the true similarity value between the hemispheres would be lower than the permuted similarity values, suggesting that the hemispheres are significantly different. As in previous examples, in each of 1000 permutations, the left- and right-hemisphere labels were exchanged for 50% of the participants that were randomly selected for each permutation. Then, a variant overlap map was created by summing the number of variants present at each vertex across participants. Using this overlap map, a correlation value was again obtained to quantify the overall similarity in variant frequency between the pseudo-left and pseudo-right hemispheres. Because we hypothesized that the left and right hemispheres would be significantly different in variant distribution, we then calculated how many of the correlation values from the 1000 permutations fell below the true correlation value to obtain a significance score. The significant threshold was set at $p \leq .025$ at either end of the distribution for a two-tailed test. This analysis was replicated in nine MSC participants (Appendix B).

We conducted an additional post hoc test to identify the locations that were most different across the two hemispheres. For this test, a difference map was created by subtracting the frequency of variants at each vertex in the right hemisphere from its homotopic pair in the left hemisphere. Significant locations in this difference map were identified through a permutation-based approach with cluster correction to correct for multiple comparisons. Specifically, across 1000 iterations, the left- and right-hemisphere labels were permuted by participant and used to create a variant overlap map. For each permutation, a vertex-by-vertex difference map between the pseudo-left and pseudo-right hemispheres was created. We then thresholded each map at 5% difference (~19 participants in the HCP subsample of 384 participants) and calculated the size of any clusters of variants that exceeded this threshold, creating a distribution of cluster sizes. Clusters in the true difference map were then compared with this permuted distribution of cluster sizes; clusters larger than 95% of the clusters obtained through permutation were interpreted as significant. Additional cluster thresholds (3% and 10% difference) were tested and included in Appendix C to show the robustness of results to this threshold choice.

Network Asymmetries across Hemispheres

We then examined if specific networks showed asymmetries in the amount of cortical territory that was labeled as variants, or idiosyncratic regions, across the two hemispheres. To do this, we first identified each participant's variant vertices and separated them by network to which they were assigned. Then, we calculated the surface area across variants

using the *wb_command* function -*surface-vertex-areas* on the Conte69 group-average midthickness cortical surface (Glasser & Van Essen, 2011). This variant surface area was then divided by the total surface area of the corresponding hemisphere to account for slight differences in hemisphere size. We then calculated a difference score (by network) for each participant, where the variant territory assigned to a network in the right hemisphere was subtracted from the variant territory that was assigned to the network in the left hemisphere. The difference scores for all participants were then averaged to obtain a mean difference score for each network. To test for significance, we again used a permutation approach, where we randomly switched the left- and right-hemisphere labels on a participant level and recalculated average difference scores for the surface area of variant territory assigned to each network. This was repeated 1000 times to generate full null distributions for each network. We compared the true difference scores to these null distributions to assess significance. The significance threshold was set at $p \leq .025$ at either end of the distribution for a two-tailed test. We again used FDR correction for multiple comparisons across 14 comparisons for each network.

To contextualize asymmetries in network variants relative to the patterns seen in the group average, we examined the symmetry of the size each network in a group average using the WashU 120 reference group (WashU 120; see Appendix D for results of this comparisons in two additional group averages: MSC and subsample of 384 HCP participants). To do this, we calculated the difference between the proportion of surface area that each network accounts for across the two hemispheres. We then compared these group-average network asymmetries with the asymmetries seen in variant surface area in each hemisphere (calculated as described above).

Analysis of Network Variant Asymmetries across Handedness Groups

We next investigated the potential relationship between hemispheric asymmetries in individual differences and dominant handedness, which is itself lateralized in most individuals and has been linked to other relatively lateralized functions such as language production (Perlaki et al., 2013; Knecht et al., 2000). We repeated the previous analyses for left- and right-handers separately. HCP participants in a sample of 752 individuals were divided into handedness groups according to their Edinburgh Handedness Inventory laterality coefficient (LQ; Oldfield, 1971). Left-handers and right-handers were determined to be so if their LQ was between −100 and −41, and 41 and 100, respectively. For each handedness group, we repeated the process of obtaining hemispheric difference scores for total variant territory, average variant size, and number of variants. The hemispheric differences (left − right hemisphere) for all members of each handedness group were then averaged and compared between left- and right-handers. We assessed significance of the handedness effect using permutation testing. In this case, we permuted the handedness group labels. Handedness labels for all participants were shuffled, retaining the size of each handedness group (i.e., 40 random participants were labeled left-handers, and 670 participants were labeled right-handers). For each permutation, we compared the difference scores between the pseudo-left- and pseudo-right-handers. This process was then repeated 1000 times to obtain a distribution of comparisons between groups. The true difference score was then compared with that null distribution to assess whether left- and right-handers

differed from each other in the different variant properties described here. Under the null hypothesis that left- and right-handers are not significantly different, shuffling the handedness group labels would yield difference scores approximately equivalent to the true difference score between left- and right-handers. If handedness was associated with altered variant asymmetries, our hypothesis was that the true difference score would fall in the tails of the null distribution.

This process was also used to compare left- and right-handers in the network assignment of variants. To compare left- and right-handers in the spatial distribution of variants, we again used permutation testing. For each of 1000 permutations, we randomly selected 40 individuals to be labeled as pseudo-left-handers and 670 individuals to be labeled pseudo-right-handers and obtained variant frequency maps as described above. The frequency maps for left- and right-handers were then compared using spatial correlation in each permutation, creating a null distribution of similarity values. The true correlation value between the variant frequency maps of left- and right-handers was then compared with this null distribution to determine significance. The significance threshold was set at $p \leq .025$ at either end of the distribution for a two-tailed test.

RESULTS

Lateralization of structure, function, and behavior are thought to occur as a consequence of multiple factors, including evolutionary, developmental, experiential, and pathological variables (see Toga & Thompson, 2003, for a review). Hemispheric asymmetries exist at all levels of brain organization, including large-scale brain systems. Here, we examined whether hemispheric asymmetries are present for network variants: focal regions of high dissimilarity between an individual's functional network pattern and that of a group average. Asymmetries in these idiosyncratic network variants could provide insight into the nature of individual differences in brain organization and how they arise. Thus, here we compare the properties of network variants between the two hemispheres.

The publicly available HCP data set was used for primary analyses in this article. This data set contains relatively high amounts of resting-state data for a large sample ($n = 384$) of young adults. The MSC, a smaller but highly sampled data set ($n = 9$ individuals with 10 sessions each), was used to replicate findings of asymmetries in spatial distribution. We examined four properties of network variants. (1) First, we assessed asymmetries in the average size, number of variant regions, and the overall variant territory in each hemisphere. (2) Next, we compared the spatial distribution of variants across hemispheres. (3) Then, the amount of variant territory associated with different networks was also compared across hemispheres. (4) Lastly, we provide a deeper examination of the relationship between network variant asymmetries and handedness, a prominent behavioral asymmetry.

Average Frequency and Size of Network Variants Differ Significantly across Hemispheres

To better understand the nature of hemispheric asymmetries in individual differences in brain organization, we examined whether variants tend to be bigger or appear more frequently in one hemisphere over the other. On average, network variants were significantly bigger on the right hemisphere compared with the left ($p < .001$ based on permutation

testing; Figure 2A; left hemisphere = 236.1 mm^2, right hemisphere = 285.3 mm^2). There was also significantly more variant surface area in the right hemisphere compared with the left ($p < .001$; left hemisphere = 2564.5 mm^2, right hemisphere = 2978.9 mm^2; Figure 2B). We found a small but significant difference in the number of variants in each hemisphere, with the left hemisphere showing slightly more variants than the right ($p = .002$, Figure 2C; left hemisphere = 11.16 variants, right hemisphere =10.64 variants; however, this result, unlike the others, was affected by choices in processing the variant subunits; see Appendix A). These results indicate that the right hemisphere exhibits more variable functional architecture, with bigger variants and more overall variant surface area. Although variants in the left hemisphere were slightly more numerous, this effect was weaker and more affected by processing choices.

Spatial Distribution of Variants Differs Significantly across Hemispheres

A relative lateralization can be observed in visualizations of the spatial distribution of network variants from past work (Figure 3A; see also Figure 3 in Seitzman et al., 2019). This difference is most apparent in the lateral frontal cortex and near the TPJ. Here, we tested whether this observed difference is significant by quantifying the similarity of variant spatial distributions between the left and right hemispheres.

Overlap maps of network variants were created for each hemisphere across participants in the HCP data set (Figure 3A). The similarity in spatial distribution of network variants was compared between the two hemispheres using spatial correlation. This true similarity was then compared with those obtained across permuted comparisons (see Methods). The results of this analysis indicate that the spatial distribution of network variants differs significantly across the two hemispheres (Figure 3B; $p < .001$, true similarity between the left and right hemispheres: $r = .74$, mean permuted similarity: $r = .99$). This finding was replicated using the MSC data set (Appendix B; $p < .001$, true similarity: $r = .39$, mean permuted similarity: $r = .52$; note that, here, correlations between all spatial distributions are substantially lower, likely because of the smaller sample size of the MSC data set).

To examine the specific locations where left and right hemispheres differ, we then did a second-level test where we subtracted the frequency of variants at each vertex in the right hemisphere from its homotopic vertex in the left hemisphere. A permutation-based cluster correction was conducted to identify locations of significant difference between the hemispheres (see Methods). This analysis shows that variants appear more frequently in the frontal operculum, angular gyrus, and superior medial frontal cortex in the right hemisphere and in the supramarginal gyrus, superior anterior frontal gyrus, and anterior portions of the medial-temporal gyrus in the left hemisphere (Figure 3B). This result was replicated using a smaller sample with high amounts of data per participant (MSC). The results of this replication analysis show a similar spatial distribution and regions of difference, though because of the small sample size, clusters were sparser (Appendix B).

Hemispheric Asymmetries in the Network Assignment of Variants

Network variants, by definition, are deviations from the canonical organization of a given functional network, associated with an atypical network for that location. Next, we explored

how variants associated with specific networks differed between the hemispheres. First, each variant region was matched to one of 14 canonical networks using a template-matching procedure based on its seed map correlation pattern (Figure 1D; see Methods). We then contrasted the extent of variants associated with each network in the left and right hemispheres.

Given the large asymmetries in variant territory between the two hemispheres, we focused first on whether variants of specific networks differed between the two hemispheres. Eight networks showed significant differences after FDR correction for multiple comparisons across 14 networks. Networks with more variant territory in the left hemisphere included the language network ($p < .004$) and somatomotor lateral network ($p < .001$), whereas those with more variant territory in the right hemisphere included the default mode ($p < .001$), frontoparietal ($p < .001$), dorsal attention ($p < .02$), cingulo-opercular ($p < .001$), parietal memory ($p < .004$), and parietal occipital ($p < .001$) networks (Figure 4). Thus, hemispheric asymmetries exist in variants, but the direction of this asymmetry depends on the specific network. Moreover, some networks are more likely to exhibit expanded idiosyncratic territory in the left hemisphere, such as the language and somatomotor network, whereas other higher cognitive networks are more likely to show idiosyncratic territory in the right hemisphere, like the default mode and cingulo-opercular networks.

Note that qualitatively similar results were also seen when asymmetries were compared for the number of variants, rather than territory covered. In this case, we found significant differences for seven of networks. Variants were more commonly found in the left hemisphere for the visual ($p < .001$), language ($p < .001$), somatomotor lateral ($p < .001$), and MTL ($p < .01$) networks and in the right hemisphere for the DMN ($p < .001$), cingulo-opercular ($p < .01$), and PMN ($p < .02$). Given the more robust findings associated with variant territory differences, we focus primarily on these comparisons moving forward.

Some of the networks that exhibit significant asymmetries in variants have been linked to functions or behaviors proposed to be differentially associated with the two hemispheres. For example, the language network has been shown to be left-hemisphere dominant in most individuals studied using precision approaches (Braga et al., 2020). Similarly, the DMN has been linked to episodic memory retrieval (Andrews-Hanna, Saxe, & Yarkoni, 2014; Andrews-Hanna, Reidler, Sepulcre, Poulin, & Buckner, 2010), a function that is hypothesized to be relatively right-lateralized (Desgranges, Baron, & Eustache, 1998; Tulving, Kapur, Craik, Moscovitch, & Houle, 1994).

Here, we looked in more detail at the spatial distributions of network variants for those that showed significant asymmetries (Figure 5). Note that these maps are not cluster-corrected for significance but are instead used as an exploratory visualization of where the differences in variants for each network occur.

The language network was associated with more variant territory in the left hemisphere, especially on the supramarginal gyrus and pars opercularis, adjacent to group-average language network regions. The somatomotor-lateral network showed the highest differences in a region on the inferior precentral gyrus, where variant frequency was significantly higher

in the left hemisphere. The cingulo-opercular network was associated with more variants in the right hemisphere, especially in a superior frontal area anterior to the precentral gyrus, further from its typical distribution. The default network had more variants in the right hemisphere, especially in regions adjacent to typical default locations along the superior frontal sulcus and in some regions along the operculum and caudal pre-frontal cortex. The frontoparietal network shows a prominent difference in an anterior portion of the medial frontal cortex, where it exhibits increased likelihood of variant territory in the right hemisphere compared with the left.

Relationship between Asymmetries in Network Variants and Network Size

To contextualize the asymmetries in variants for each network, we asked whether there are asymmetries in the size of the networks found in the group-average network map (Figure 6 inset). We show that, even in the group-average, functional networks vary in the degree to which they show asymmetries (Figure 6A). Although most networks are relatively symmetric, the default mode and language networks were larger in the left hemisphere by 10%, equivalent to 1100 mm^2, and 9%, equivalent to 349 mm^2, respectively. The frontoparietal (yellow dot in Figure 6A) and cingulo-opercular networks (purple dot in Figure 6A) were larger in the right hemisphere by 14%, or 686 mm^2, and 8%, or 606 mm^2, respectively. Similar results were seen in group-average networks from other data sets (Appendix D; e.g., note that across group averages the DMN consistently shows the same pattern of large difference, with more surface area in the left hemisphere).

These group-average network asymmetries can then be contrasted with the differences in variant surface area for each network (Figure 6B). For example, if a network is relatively symmetric in the group average but it exhibits more variant territory in one hemisphere compared with the other, this may suggest that individual differences in that network lead it to be more asymmetric within many people. This appears to be the case for the dorsal attention and parietal memory networks. Alternatively, if a network shows hemispheric differences in the group average, variants in one hemisphere could either magnify that asymmetry (if variants are ipsilateral to the group-average asymmetry), or it could counter it (if variants are instead more common in the contralateral hemisphere of the group-average asymmetry). We see apparent examples of both cases: for instance, cingulo-opercular, fronto-parietal, and language variants occur primarily ipsilateral as their group-average asymmetries, whereas default mode variants appear primarily contralaterally (Figure 6C). A similar pattern was observed when comparing the average number (rather than surface area) of variant regions associated with specific networks across the two hemispheres (Appendix E).

Relationship between Handedness and Hemispheric Asymmetries

Handedness is a prominent behavioral trait that shows natural variance in the direction and degree of asymmetry throughout the population. Handedness has been shown to be related to other lateralized functions such as language. Because of this, we looked into asymmetries in network variants as a function of handedness in 40 left-handers and 670 right-handers from the HCP data set (see Methods for handedness definition). The number, size, and spatial distribution of variants, as a whole, showed no significant differences between the

two handedness groups. Interestingly, however, the two groups differed significantly in the specific networks that show asymmetries in their variants. We found significant interactions of handedness by hemisphere for two networks, namely, the cingulo-opercular ($p = .004$ based on permutation testing, FDR corrected for multiple comparisons) and frontoparietal ($p = .006$) networks (Figure 7A)—two important networks for cognitive control. These interactions reveal that whereas right-handers do not differ significantly in their number of frontoparietal variants across hemispheres, left-handers show an increased number of frontoparietal variants in their left hemisphere ($p = .006$; Figure 7B). In contrast, whereas right-handers have significantly more cingulo-opercular variants in their right hemisphere ($p < .001$; Figure 7C), left-handers do not show a significant difference. These findings add to the evidence suggesting that network variants are linked to behavior, and in particular, that asymmetries in network variants are related to asymmetrical functions and behaviors.

DISCUSSION

The results described in this article indicate that the properties of network variants differ across the two cerebral hemispheres. Generally, the right hemisphere shows larger variants and more total variant territory. Variants were slightly more numerous in the left hemisphere, but this effect was small and dependent on specific preprocessing steps. These findings suggest that the right hemisphere exhibits a higher degree of variability in functional organization than the left.

A deeper examination of where specifically the two cerebral halves differ showed that the left hemisphere exhibits higher variant frequency on the supramarginal gyrus, superior anterior frontal gyrus, and anterior portions of the medial-temporal gyrus, whereas the right hemisphere appears to have more variants on the orbital and triangular parts of the inferior frontal gyrus, angular gyrus, and superior caudal frontal cortex. These asymmetries also varied by network, with some networks exhibiting more variants in the left hemisphere, whereas others are more likely to have variants in the right hemisphere, and yet other networks showing a more even distribution of variants. Although some of these asymmetries in network variants built on the asymmetries seen in group-average network organization, others showed asymmetries in opposing directions. Finally, asymmetries in some networks (cingulo-opercular, frontoparietal) varied between left- and right-handers, suggesting a link to functional traits. Jointly, these findings provide evidence that idiosyncratic network variants exhibit hemispheric constraints in their development. These constraints may be linked to differences in associated cognitive/behavioral functions.

Individual Differences in Brain Networks Add to or Counter Asymmetries Seen in Group Averages

The distribution of network variants for eight functional networks differed across hemispheres, suggesting that these networks show increased variability in one hemisphere compared with the other.[1] Specifically, the default mode, cingulo-opercular, frontoparietal, dorsal attention, parietal occipital, and parietal memory networks showed higher frequency

[1]Notably, our analyses did not test if the spatial location of regions was directly homologous; most analyses compared omnibus properties of the two hemispheres. In one case, we tested the spatial point-by-point correspondence of idiosyncratic variants between

of variants in the right hemisphere, and the language and somatomotor-lateral networks exhibited higher frequency of variants in the left hemisphere.

Our analyses in the group average showed that cortical networks, on average, show slight differences in the amount of cortical territory that they cover across the two hemispheres. Thus, a hemispheric asymmetry in variants associated with a network may either magnify or counteract the typical “group-average” pattern. For example, the language and cingulo-opercular networks both have more overall variant territory (and increased number of variants) in the ipsilateral hemisphere as their group-average asymmetry, suggesting that variants of these networks tend to manifest as a greater degree of lateralization in some individuals (this was also true to some degree for the somatomotor lateral network, though because this system is relatively small, the hemispheric differences in surface area in the group average were also small). In contrast, some networks exhibit more variant territory in the contralateral hemisphere relative to the group average dominance, such that the initial asymmetry in surface area may be regressed in some individuals. This appears to apply to the default mode and parietal occipital networks.

One network with expanded variants in the left hemisphere was the language network. Figure 6 shows that the language network appears to be slightly larger in the left hemisphere in group averages. The relatively large number of language network variants in the left hemisphere points to two important aspects of this network: (1) It is consistent with prior observations that this network tends to be relatively left-lateralized in most individuals (Braga et al., 2020), and (2) that key regions of this network are highly variable across people (Fedorenko & Blank, 2020; Fedorenko et al., 2012). That group-average representations do not strongly reflect the leftward lateralization of the language network indicates that the group-average language network may be failing to capture important areas that exhibit a higher degree of variability across individuals (Lipkin et al., 2022; Dworetsky, Seitzman, Adeyemo, Neta, et al., 2021). These highly variable regions that are not reflected in the group average would then be labeled network variants, explaining the asymmetry of language variant territory found in our analyses.

In contrast, core regions of the DMN exhibit high concordance across individuals (Dworetsky, Seitzman, Adeyemo, Neta, et al., 2021). This network also shows a relationship with putatively asymmetrical functions, such as episodic memory and retrieval (Rugg & Vilberg, 2013; Desgranges et al., 1998). As we show here, the DMN is associated with increased surface area in the left relative to the right hemisphere in group averages. However, within single individuals, this network showed expanded variant territory (and variant numbers) in the right hemisphere compared with the left. In contrast to the lateralization of the language network, the higher number of DMN variants in the right hemisphere may indicate a relative “renormalization” of this network in some individuals. This network has been associated with a range of introspective functions including episodic retrieval, future planning, and social tasks like mentalizing, likely fractionating into separable subcomponents (DiNicola, Braga, & Buckner, 2020; Buckner & DiNicola, 2019;

the two hemispheres; however, network variants do not necessarily correspond to distinct regions, and thus, the presence of variant correspondence across the hemispheres cannot alone be taken as conclusive evidence of homology.

Andrews-Hanna et al., 2014; Mars et al., 2012; Saxe & Kanwisher, 2003). The region where we observed a higher frequency of variants on the right hemisphere, around the angular gyrus, in particular, has previously been implicated in theory of mind (Andrews-Hanna et al., 2014). Further research is necessary to confirm the implications of variant asymmetries for these different functions associated with the DMN.

The frontoparietal network was associated with increased variant territory in the right hemisphere as well as an asymmetry of variants associated with this network in left-handers (though this asymmetry was not observed in the number of variants in the overall group). The frontoparietal network is an important cognitive control network that is highly integrated with other large-scale systems and is thought to provide rapid and flexible modulation of other networks (Marek & Dosenbach, 2018). This network has previously reported to show strong specialization within each hemisphere (Wang et al., 2014) and tends to subdivide into left and right subnetworks in group maps (Smith et al., 2009), with the left-hemisphere network showing early responses and the right-hemisphere network showing late onsets with prolonged responses during decision-making (Gratton et al., 2017). Each subnetwork also flexibly couples with either the default mode or dorsal attention networks (Spreng, Sepulcre, Turner, Stevens, & Schacter, 2013; Spreng, Stevens, Chamberlain, Gilmore, & Schacter, 2010). Thus, it has been hypothesized that the left and right frontoparietal subnetworks contribute to different sets of functions through their interactions with distinct networks. The frontoparietal network is also linked to a particularly high number of variants relative to sensorimotor systems (Seitzman et al., 2019). An increased extent of variant territory associated with this network may suggest a larger link to rightward-asymmetrical functions. However, the finding that left-handers, unlike right-handers, show a significant asymmetry in this network suggests that the frontoparietal network exhibits systematic differences across handedness groups that may be averaged out due to left-handers being a minority (and often excluded) from most samples.

Variant Asymmetries Inform Us of Developmental Constraints on Individual Brain Networks

What factors may give rise to asymmetries in idiosyncratic network variants? The cortical organization of the brain exhibits variation across individuals in the size, shape, and spatial topography of functional networks. Although size and spatial topography of networks has been shown to be moderately heritable (Anderson et al., 2021), variability in cortical regions may also arise due to developmental events that affect the way that functional systems are organized on the cortex (Krubitzer & Seelke, 2012). For example, signaling cascades direct the graded expression of transcription factors that regulate patterning of the cortex (O'Leary, Chou, & Sahara, 2007; Sur & Rubenstein, 2005), and alterations in their pattern of expression can result in alterations to the size and position of cortical areas (Garel, Huffman, & Rubenstein, 2003; Fukuchi-Shimogori & Grove, 2001). Additionally, experiential factors have been shown to influence cortical organization. In cases of congenital blindness and deafness, the change in relative patterns of sensory-driven stimulation can lead to alterations in sensory domain allocation, cortical field size, and cortical and subcortical connectivity (Striem-Amit et al., 2015; Hunt, Yamoah, & Krubitzer, 2006; Kahn & Krubitzer, 2002). In congenital blindness, the absence of visual experience seems to lead to increase

intraindividual variability in functional connectivity patterns, suggesting that sensory experience imposes some consistency in brain organization (Sen et al., 2022). In normative development, experience guides the development of face- and scene-responsive areas in the central and peripheral portions of the retinotopic map, respectively (Arcaro & Livingstone, 2017; Srihasam, Vincent, & Livingstone, 2014; Downing, Jiang, Shuman, & Kanwisher, 2001; Kanwisher, McDermott, & Chun, 1997). Interestingly, hemispheric dominance for certain functions is thought to arise as a result of competition for representational space. Because of proximity to language areas, the ventral occipitotemporal cortex in the left hemisphere is ideally situated for orthographic processing and as such becomes specialized for word perception, which may lead to a rightward asymmetry for face perception given lower competition in that hemisphere (Dundas, Plaut, & Behrmann, 2015; Behrmann & Plaut, 2013). Thus, the organization of brain regions and networks can be shaped by biological, environmental, and developmental factors.

A recent compelling hypothesis describes a potential mechanism that guides the development of functional networks at the individual level. The expansion–fractionation–specialization hypothesis (DiNicola & Buckner, 2021) proposes that the disproportionate expansion of association areas in the human brain has provided large zones of cortex that share a distributed anatomical connectivity motif, where frontal, temporal, and parietal areas are highly interconnected. Early in development, association cortex may exhibit a proto-organization characterized by a coarse network with poorly differentiated anatomical connectivity that, as developmental events occur and experience accumulates, fractionates into multiple networks that specialize in different functions (DiNicola & Buckner, 2021). Which function each network is associated with is determined through competitive activity-dependent processes but may be biased by differences in anatomical connectivity to regions that are relevant to its function (Buckner & DiNicola, 2019; Braga & Buckner, 2017). For example, language production regions may be “anchored” by orofacial motor regions important for speech because of their functional relationship and may therefore frequently develop adjacent to each other (Braga et al., 2020; Krubitzer, 2007). The result of this fractionation and specialization process are multiple fine-grained networks, with networks important for flexible cognitive functions being farthest from unimodal regions (Huntenburg, Bazin, & Margulies, 2018; Buckner & Krienen, 2013).

Hemispheric asymmetries may reflect another form of specialization within this process. Transmodal functional systems that support flexible cognitive functions require integration between areas that are far apart (Mesulam, 1998), but interhemispheric connections incur extra processing costs. A hypothesis for the evolutionary advantage of lateralization in the CNS proposes that this motif arose to facilitate performing tasks in parallel, as well as fast processing for important functions such as language, which requires rapid sequential processing, and visuospatial processing, which requires rapid identification of objects and their relations (Güntürkün & Ocklenburg, 2017). This is supported by studies showing that both animals (Rogers, Zucca, & Vallortigara, 2004; Güntürkün et al., 2000) and humans (Chiarello, Welcome, Halderman, & Leonard, 2009; Everts et al., 2009) perform better at doing tasks in parallel if they show increased lateralization of relevant functions. Thus, lateralization of networks may arise to decrease redundancy of processing (Esteves, Lopes, Almeida, Sousa, & Leite-Almeida, 2020; Levy, 1977). This may be especially important for

functions that require fast and serial processing, such as language. Therefore, the advantage of lateralization likely depends on the network and the processes that it supports.

Lateralization of functional networks may be biased by qualitative differences in the architecture of the hemispheres, such as differences in cortical microcircuitry. For example, pyramidal cell dendrites in the right hemisphere form, on average, more long-range connections compared with the left hemisphere (Hutsler & Galuske, 2003). Indeed, the wiring patterns of the left hemisphere seem to be more suitable for specific, core linguistic processing than those observed in the right hemisphere, which in general is more interconnected (see Box 1 in Jung-Beeman, 2005). If a function or system becomes lateralized throughout development, a unique combination of genetic influences, developmental events, and idiosyncratic experiences will likely give rise to differences in the spatial topology of the network as it fractionates and specializes in the dominant hemisphere, giving rise to network variants that are more prominent in that hemisphere. Interestingly, association areas that show disproportionate expansion during evolution, and from infancy to adulthood (Hill et al., 2010), overlap significantly with areas of asymmetry in the degree of within-hemispheric functional connectivity (hemispheric specialization; Wang et al., 2014). Thus, asymmetries in network variants may reflect a form of specialization of these functional systems that may arise as a consequence of qualitative differences in the way that the two hemispheres process information.

Asymmetries in Individual Differences May Be Markers for Healthy and Pathological Differences in Brain Function

Previous research suggests that variability of cortical regions (e.g., Verghese, Kolbe, Anderson, Egan, & Vidyasagar, 2014; Schwarzkopf, Song, & Rees, 2011) and spatial topography of networks (Kong et al., 2019; Lake et al., 2019; Bijsterbosch et al., 2018; Shen et al., 2017) may have implications for behavior and cognition. Here, we found that asymmetries in two networks important for cognitive control, the cingulo-opercular and frontoparietal networks, differed between left- and right-handers. Interestingly, the cingulo-opercular network has been implicated in motor control in recent reports where it showed altered functional connectivity in response to disuse of motor circuits related to participants' dominant hand (Newbold et al., 2021). Thus, understanding the properties of network variants may help elucidate brain–behavior relationships. An important reason for characterizing brain–behavior relationships in normative samples is to understand how alterations may lead to different forms of pathology. The trait-like characteristics of variants and relationship to behavioral measures suggests their potential utility as biomarkers for atypical brain function associated with altered cognitive function.

Our findings demonstrate the existence of asymmetries in the properties of network variants in a sample of healthy young adults. However, some pathological conditions exhibit atypical asymmetries in brain function that could potentially alter the pattern of asymmetries observed in our sample. For example, autism spectrum disorder has been associated with altered lateralization of language (Floris et al., 2021; Jouravlev et al., 2020; Liu et al., 2019; Escalante-Mead, Minshew, & Sweeney, 2003) as well as handedness and cortical structure in previous reports (Lindell & Hudry, 2013). This atypical language lateralization in autism

has been shown to be largely independent of other asymmetries, as other large-scale systems (namely, the DMN and "multiple demand" or frontoparietal networks) were not found to exhibit atypical asymmetries (Nielsen et al., 2014). Similarly, schizophrenia has been linked to differences in cerebral asymmetries (Oertel-Knöchel & Linden, 2011), including asymmetries of language and handedness (Artiges et al., 2000; Crow, Done, & Sacker, 1996), as well as reduced anatomical asymmetries (Sommer, Aleman, Ramsey, Bouma, & Kahn, 2001). Thus, one theory for the cause of the disorder is delayed cerebral lateralization (Crow et al., 1996). This suggests that alterations in brain asymmetries may contribute to pathological conditions that may interfere with cognitive function. Although the properties of network variants in clinical populations remain to be uncovered, investigating whether the pattern of asymmetry associated with individual differences described here would be altered in cases of atypical lateralization associated with the aforementioned conditions could potentially lead to identification of characteristics by which clinical populations can be stratified according to neurobiological profiles.

Hemispheric asymmetries may be altered by nonpathological factors as well, such as normative aging (Szaflarski, Holland, Schmithorst, & Byars, 2006; Cabeza, 2002; Bäckman et al., 1997; Cabeza et al., 1997). This decrease in hemispheric asymmetries may arise as a compensatory mechanism (Reuter-Lorenz & Cappell, 2008; Cabeza et al., 1997) or dedifferentiation processes (Li & Lindenberger, 1999). In addition to studying network variants and their asymmetries in clinical populations, it would be interesting to track their asymmetries throughout the lifespan. Changes in the asymmetries of network variants would suggest that their presence is under the influence of activity-dependent processes. Furthermore, understanding age-related changes to the properties of network variants could yield a better understanding of their potential application for therapeutic approaches and their relationship with lateralized functions and disorders. If network variants are trait-like features of brain organization that reflect cognitive differences across individuals, measuring their asymmetries and how they change as a function of pathological conditions and age may serve to track disease processes and age-related cognitive decline and dementias.

Limitations and Future Directions

This work led to an increased understanding of how individual differences in functional connectivity compare across the two hemispheres. However, we note some limitations and opportunities for future investigations. First, the analyses described in this report found asymmetries in the frequency of variants in perisylvian regions. These regions have previously been found to be highly anatomically variable across individuals, though asymmetries tend to be small in magnitude (Van Essen, Glasser, Dierker, Harwell, & Coalson, 2012). Although we did not examine the relationship between anatomical variability and location of network variants in this study, previous reports have shown that the locations of network variants do not correlate with measures of gross anatomical deformations. Seitzman et al. (2019) showed that regions labeled as network variants do not overlap well with large deformations that occurred during surface registration within the individual, suggesting that network variants do not systematically arise due to anatomical variability (Seitzman et al., 2019). Additionally, it has been shown that individual-specific features of functional organization persist even after controlling for accuracy of anatomical

registration (Gordon, Laumann, Adeyemo, & Petersen, 2017). Future work will be needed to determine if finer-scale anatomical features, or more specialized anatomical–functional relationships, relate to asymmetries in network variants.

Second, the networks used for these analyses are an estimation based on the functional connectivity at rest of a group average. Their correspondence with task-evoked activations has not been verified at the individual level in this work, though previous evidence indicates correspondence between resting-state functional networks and task activation maps (Braga et al., 2020; Gordon, Laumann, Gilmore, et al., 2017; Tavor et al., 2016; Andrews-Hanna et al., 2014; Smith et al., 2009). It is unclear how our method for matching variants with networks would perform for an individual who diverges extremely from the group-average spatial pattern (e.g., an individual with a rightward asymmetry for language). Thus, the network labels assigned to variants here should be taken cautiously and verified functionally in the future.

Lastly, our analyses on the relationship between variant asymmetries and handedness uncovered hemispheric differences in the variants of two functional networks that are implicated in cognitive control, but the two handedness groups did not differ in other properties of variant regions. Although we relaxed our inclusion criteria (by including sets of related participants) to increase our number of left-handers, our left-handed sample was only of 40 individuals, and the disparity in size between the left- and right-handed samples was substantial. Thus, the possibility remains that handedness may be related to hemispheric differences in other network variant properties that are more subtle and may require a larger sample of left-handed individuals to uncover.

This work provides a reference point for looking at potential altered asymmetries in network variants across various conditions. Future directions might include examining the patterns of network variants in individuals suffering with disorders that exhibit altered asymmetries in the brain and older adults, where the asymmetries observed in this report may show an atypical pattern because of pathological factors, experience accumulation, or dedifferentiation of functional systems. Lastly, network variants have not been examined in the cerebellum, but asymmetries of within-hemispheric connectivity show a mirrored pattern relative to that seen in the cerebrum (Wang et al., 2014). Thus, it would be interesting to examine if this mirrored pattern holds for asymmetries seen in cerebellar network variants.

Conclusion

We examined hemispheric asymmetries in the properties of network variants or regions in which patterns of functional connectivity differ strongly between an individual and a group-average representation. We found that, in general, the right hemisphere has more “variant territory,” which is linked to larger variant regions. Significant asymmetries were also found in the spatial distribution of network variants, which were more prominent around the inferior frontal gyrus and the inferior parietal lobule. These asymmetries varied by network, with some networks showing asymmetries in the same direction as asymmetries in group-average network patterns and others in the opposite direction. Finally, we found significant differences between left- and right-handed participants in the asymmetries observed for variants of the cingulo-opercular and frontoparietal networks, suggesting a

relationship between network variant asymmetries and differences in behavioral traits. Jointly, these findings demonstrate that variant regions in large-scale functional networks differ systematically across the two hemispheres, indicating that they may be constrained by developmental differences and/or processes that result in functional hemispheric asymmetries. Furthermore, these findings in a sample of healthy young adults may serve as a benchmark to which we can compare future studies investigating asymmetries in network variants in conditions that have been shown to be associated with altered functional lateralization in the brain, such as aging, schizophrenia, and autism spectrum disorder.

Acknowledgments

This research was supported in part through the computational resources and staff contributions provided for the Quest highperformance computing facility at Northwestern University, which is jointly supported by the Office of the Provost, the Office for Research, and Northwestern University Information Technology.

Funding Information

Diana C. Perez, National Institutes of Health (https://dx.doi.org/10.13039/100000002), grant number: T32NS047987. Rodrigo M. Braga, National Institutes of Health (https://dx.doi.org/10.13039/100000002), grant number: 4R00MH117226. Caterina Gratton, National Institutes of Health (https://dx.doi.org/10.13039/100000002), grant number: R01MH118370.

Data Availability Statement

The data used for these analyses are publicly available and may be accessed at https://www.humanconnectomeproject.org/data/ and at https://openneuro.org/datasets/ds000224. The code used to analyze the data may be accessed at https://github.com/dianaperez25/PerezEtAl_HemAsymmetries.

APPENDIX

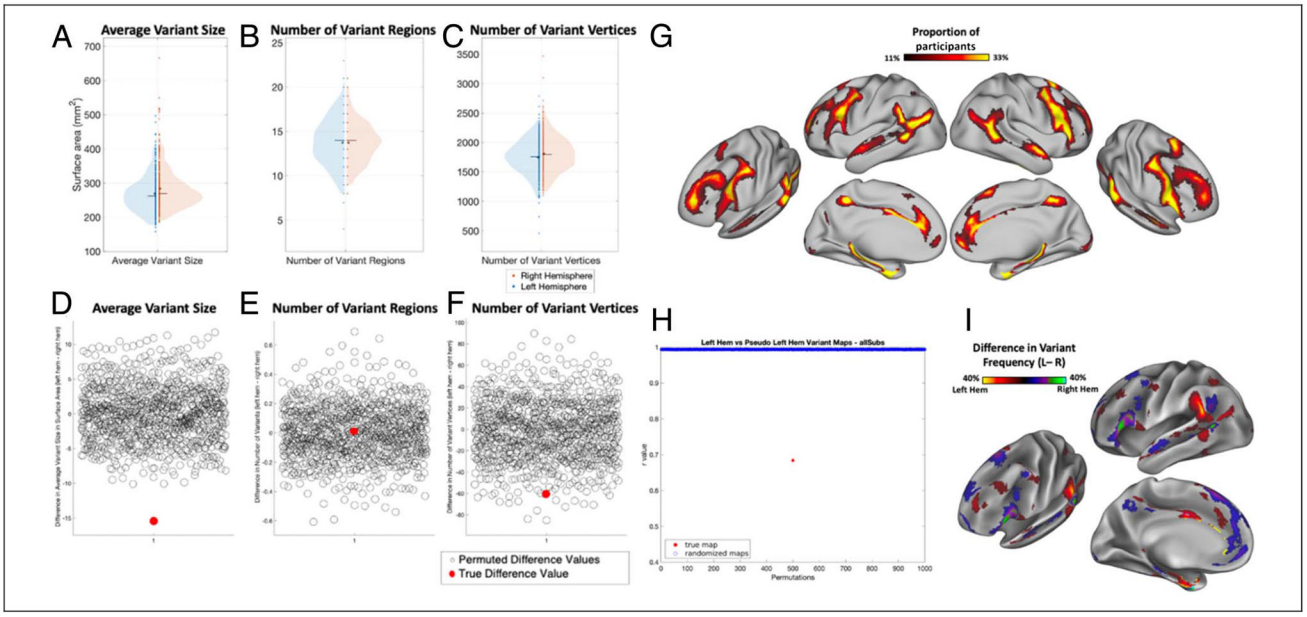

Appendix A.

Examination of hemispheric asymmetries in the properties of network variants before undergoing the refinement process (“prevariants”). (A–C) Comparisons of average variant size, number of variant regions, and number of variant vertices across hemispheres in a subsample of 384 participants from the HCP. (D–F) Results of permutation testing for significance. True difference value indicates the difference between the true left and right hemispheres. Permuted difference values indicate differences obtained by randomly flipping the left and right hemispheres of participants 1000 times. (G) Network variant overlap across participants. (H) Results of permutation testing for significance. True map indicates the correlation between variant overlap maps of the true left and right hemispheres. Randomized maps values indicate correlations between overlap maps obtained by randomly flipping the left and right hemispheres of participants 1000 times. (I) A difference map shows the regions in which the two hemispheres differ in the proportion of variant frequency. Warm colors indicate more variant overlap in left hemisphere, whereas cool colors indicate more variant overlap in right hemisphere. The spatial frequency of network variants differs significantly across the two hemispheres. Although this analysis was conducted on network variants that were defined differently than those in the main text, the general distribution and differences across the hemispheres are replicated (compare this figure with Figure 3).

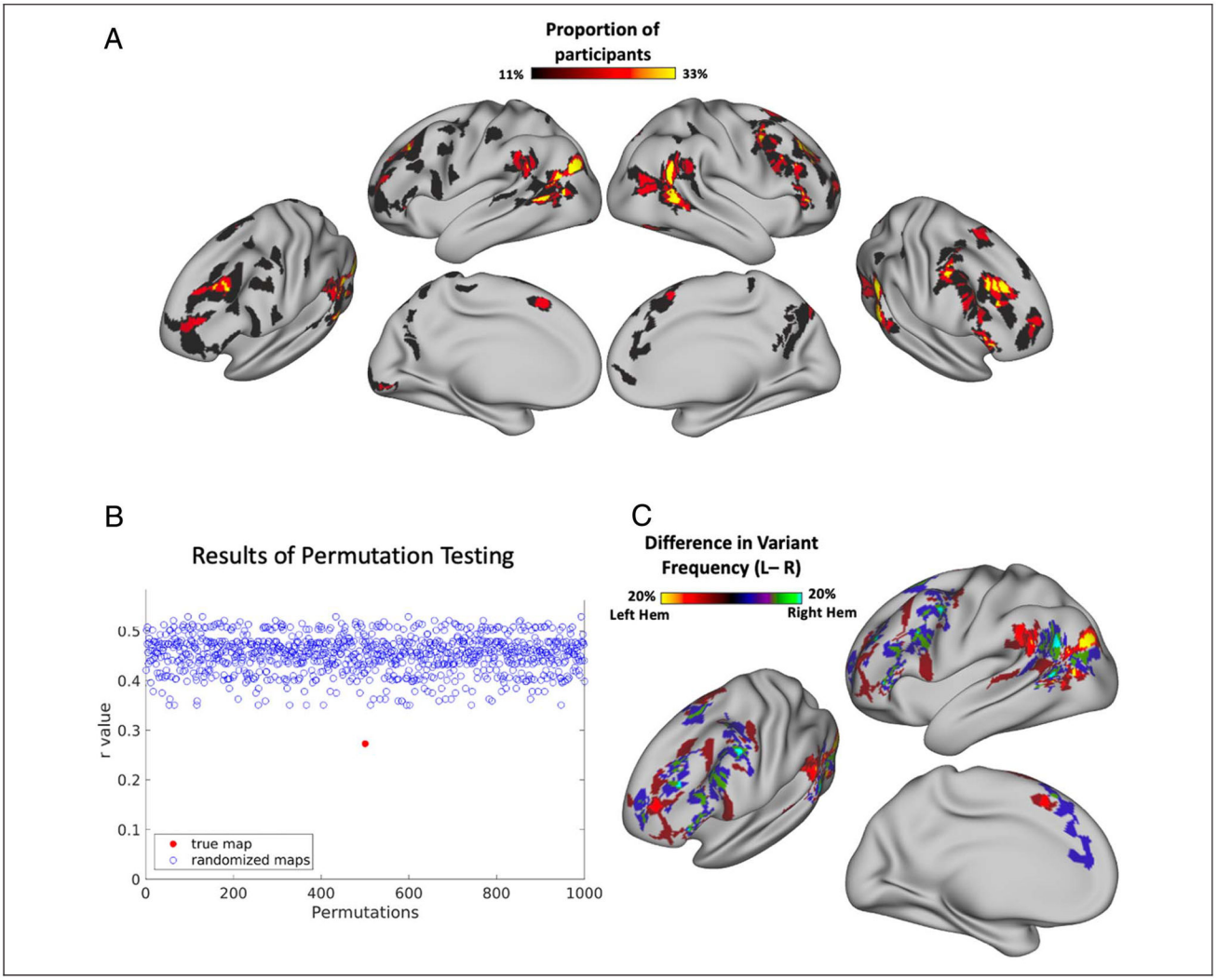

Appendix B.

Examination of hemispheric asymmetries in the spatial distribution of network variants in an independent sample (MSC). (A) Network variant overlap across nine participants from the MSC. (B) Results of permutation testing for significance. True map indicates the correlation between variant overlap maps of the true left and right hemispheres. Randomized maps values indicate correlations between overlap maps obtained by randomly flipping the left and right hemispheres of participants 1000 times. (C) A difference map shows the regions in which the two hemispheres differ in the proportion of variant frequency. Warm colors indicate more variant overlap in left hemisphere, whereas cool colors indicate more variant overlap in right hemisphere. The spatial frequency of network variants differs significantly across the two hemispheres. Although this analysis was conducted on a substantially smaller number of participants, with very different spatial and temporal scanning parameters, the general distribution and differences across the hemispheres are recapitulated (compare this figure with Figure 3). The substantially smaller sample size likely accounts for sparser clusters.

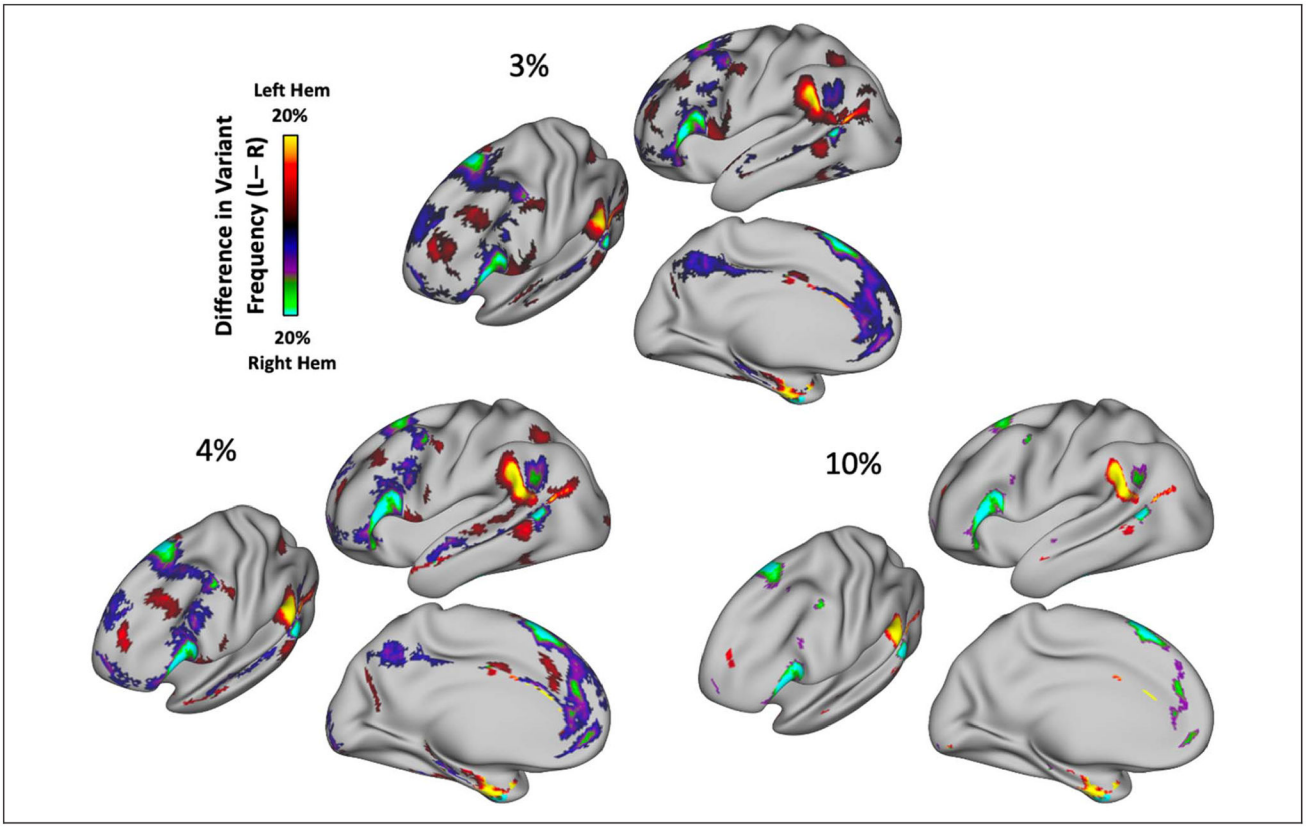

Appendix C.

Comparison of cluster correction thresholds. Three cluster difference thresholds (3%, 4%, and 10%) were tested to observe the effect of this parameter on the results. The asymmetries seen across the two hemispheres appear to be robust to the effects of this parameter; smaller clusters are lost as cluster difference thresholds are raised. For the results described in the main text, a threshold of 5% was used.

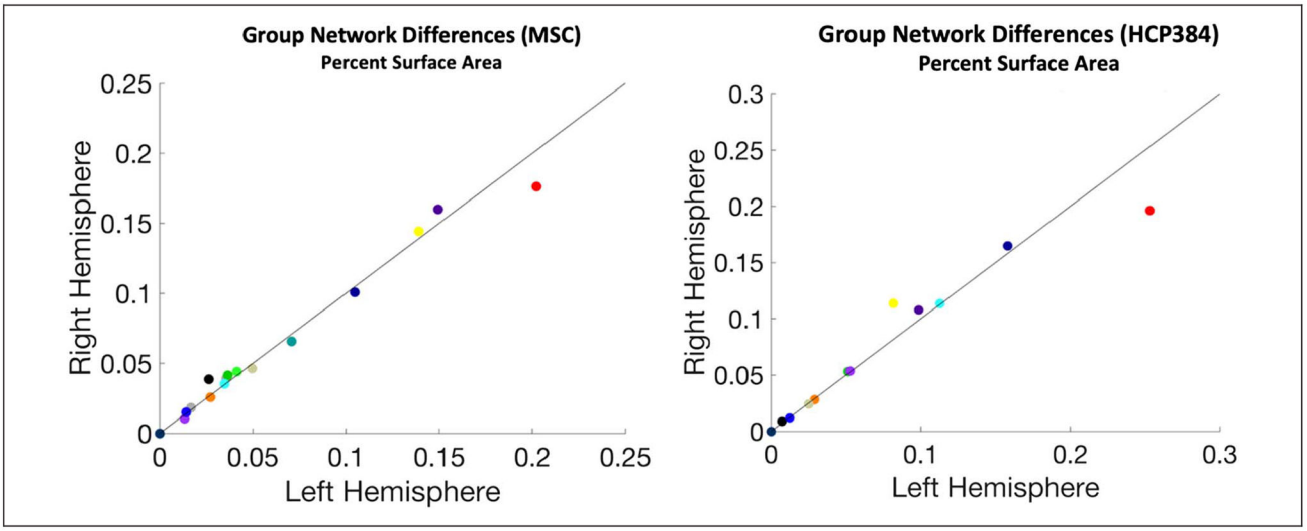

Appendix D.

Comparison of surface area across hemispheres of additional group average networks. Two group averages—the MSC and HCP (n = 384)—were examined to observe the consistency of the pattern observed in the Wash U 120 group average (see Figure 4). The DMN consistently exhibits the biggest difference in surface area, with a left-hemisphere lateralization (2.6% in MSC, 5.7% in HCP). Networks were defined using the data-drive network identification procedure InfoMap. Note that the HCP does not include the language, MTL, or T-pole group-level networks because these networks do not emerge consistently across edge density in this data set.

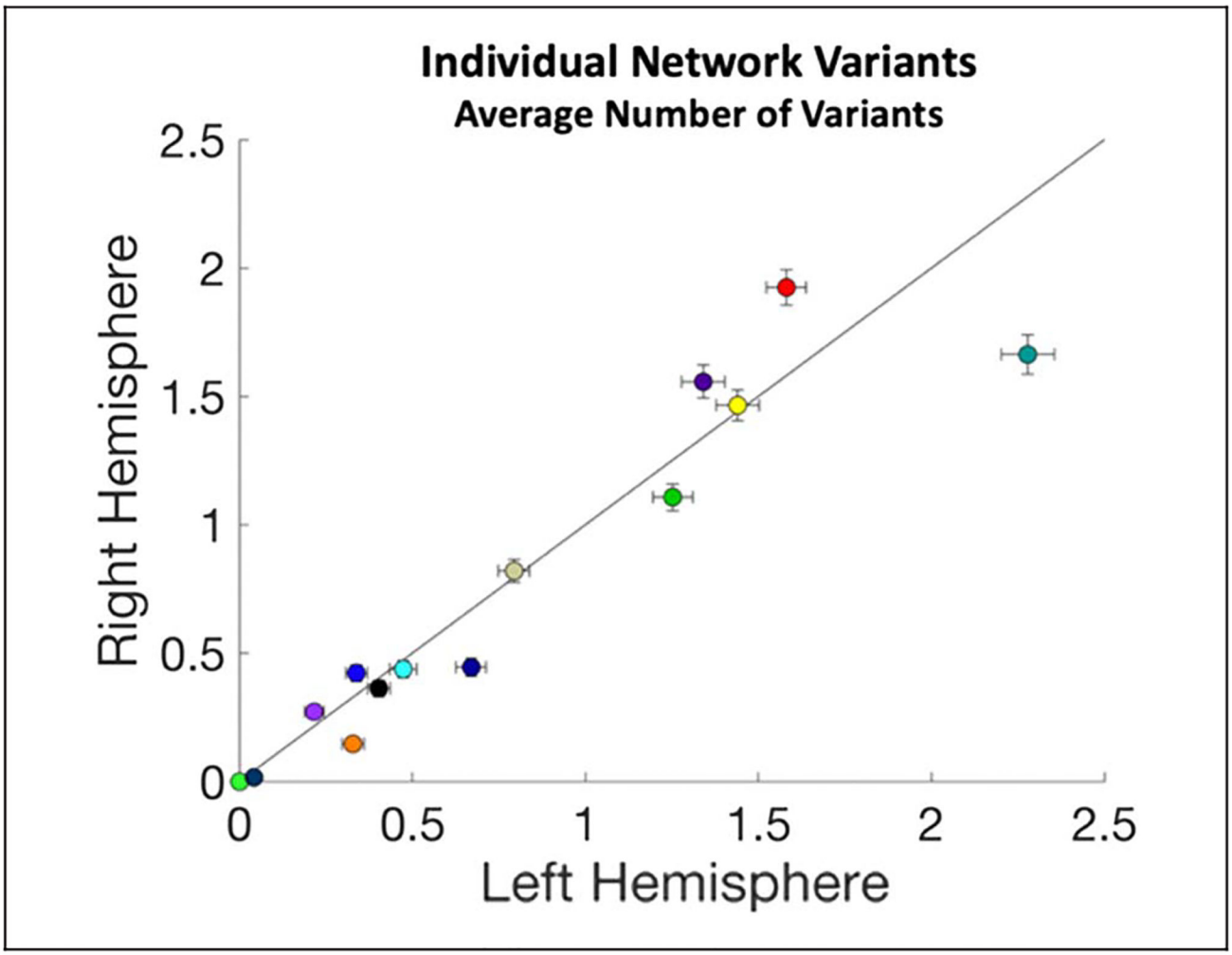

Appendix E.

Comparison of number of network variant regions across hemispheres in the HCP. The average number of variant regions associated with specific networks in the left (x-axis) and right (y-axis) hemispheres measured in the HCP (n = 384). Each color corresponds to a different network. Error bars = *SEM*.

REFERENCES

Ambekar A, Ward C, Mohammed J, Male S, & Skiena S (2009). Name-ethnicity classification from open sources. In Proceedings of the 15th ACM SIGKDD International Conference on Knowledge Discovery and Data Mining—KDD '09 (pp. 49–58). New York: Association for Computing Machinery. 10.1145/1557019.1557032

Anderson KM, Ge T, Kong R, Patrick LM, Spreng RN, Sabuncu MR, et al. (2021). Heritability of individualized cortical network topography. Proceedings of the National Academy of Sciences, U.S.A, 118, e2016271118. 10.1073/pnas.2016271118,

Andrews-Hanna JR, Reidler JS, Sepulcre J, Poulin R, & Buckner RL (2010). Functional-anatomic fractionation of the brain's default network. Neuron, 65, 550–562. 10.1016/j.neuron.2010.02.005, [PubMed: 20188659]

Andrews-Hanna JR, Saxe R, & Yarkoni T (2014). Contributions of episodic retrieval and mentalizing to autobiographical thought: Evidence from functional neuroimaging, resting-state connectivity, and fMRI meta-analyses. Neuroimage, 91, 324–335. 10.1016/j.neuroimage.2014.01.032, [PubMed: 24486981]

Anticevic A, Repovs G, Dierker DL, Harwell JW, Coalson TS, Barch DM, et al. (2012). Automated landmark identification for human cortical surface-based registration. Neuroimage, 59, 2539–2547. 10.1016/j.neuroimage.2011.08.093, [PubMed: 21925612]

Arcaro MJ, & Livingstone MS (2017). Retinotopic organization of scene areas in macaque inferior temporal cortex. Journal of Neuroscience, 37, 7373–7389. 10.1523/JNEUROSCI.0569-17.2017, [PubMed: 28674177]

Artiges E, Martinot J-L, Verdys M, Attar-Levy D, Mazoyer B, Tzourio N, et al. (2000). Altered hemispheric functional dominance during word generation in negative schizophrenia. Schizophrenia Bulletin, 26, 709–721. 10.1093/oxfordjournals.schbul.a033488, [PubMed: 10993408]

Bäckman L, Almkvist O, Andersson J, Nordberg A, Winblad B, Reineck R, et al. (1997). Brain activation in young and older adults during implicit and explicit retrieval. Journal of Cognitive Neuroscience, 9, 378–391. 10.1162/jocn.1997.9.3.378, [PubMed: 23965013]

Behrmann M, & Plaut DC (2013). Distributed circuits, not circumscribed centers, mediate visual recognition. Trends in Cognitive Sciences, 17, 210–219. 10.1016/j.tics.2013.03.007, [PubMed: 23608364]

Bijsterbosch JD, Woolrich MW, Glasser MF, Robinson EC, Beckmann CF, Van Essen DC, et al. (2018). The relationship between spatial configuration and functional connectivity of brain regions. eLife, 7, e32992. 10.7554/eLife.32992, [PubMed: 29451491]

Biswal B, Yetkin FZ, Haughton VM, & Hyde JS (1995). Functional connectivity in the motor cortex of resting human brain using echo-planar MRI. Magnetic Resonance in Medicine, 34, 537–541. 10.1002/mrm.1910340409, [PubMed: 8524021]

Braga RM, & Buckner RL (2017). Parallel interdigitated distributed networks within the individual estimated by intrinsic functional connectivity. Neuron, 95, 457–471. 10.1016/j.neuron.2017.06.038, [PubMed: 28728026]

Braga RM, DiNicola LM, Becker HC, & Buckner RL (2020). Situating the left-lateralized language network in the broader organization of multiple specialized large-scale distributed networks. Journal of Neurophysiology, 124, 1415–1448. 10.1152/jn.00753.2019, [PubMed: 32965153]

Breier JI, Simos PG, Zouridakis G, & Papanicolaou AC (2000). Lateralization of activity associated with language function using magnetoencephalography: A reliability study. Journal of Clinical Neurophysiology, 17, 503–510. 10.1097/00004691-200009000-00010, [PubMed: 11085554]

Buckner RL, & DiNicola LM (2019). The brain's default network: Updated anatomy, physiology and evolving insights. Nature Reviews Neuroscience, 20, 593–608. 10.1038/s41583-019-0212-7, [PubMed: 31492945]

Buckner RL, & Krienen FM (2013). The evolution of distributed association networks in the human brain. Trends in Cognitive Sciences, 17, 648–665. 10.1016/j.tics.2013.09.017, [PubMed: 24210963]

Buckner RL, Krienen FM, & Yeo BTT (2013). Opportunities and limitations of intrinsic functional connectivity MRI. Nature Neuroscience, 16, 832–837. 10.1038/nn.3423, [PubMed: 23799476]

Cabeza R (2002). Hemispheric asymmetry reduction in older adults: The HAROLD model. Psychology and Aging, 17, 85–100. 10.1037/0882-7974.17.1.85, [PubMed: 11931290]

Cabeza R, Grady CL, Nyberg L, McIntosh AR, Tulving E, Kapur S, et al. (1997). Age-related differences in neural activity during memory encoding and retrieval: A positron emission tomography study. Journal of Neuroscience, 17, 391–400. 10.1523/JNEUROSCI.17-01-00391.1997, [PubMed: 8987764]

Cai Q, Van der Haegen L, & Brysbaert M (2013). Complementary hemispheric specialization for language production and visuospatial attention. Proceedings of the National Academy of Sciences, U.S.A, 110, E322–E330. 10.1073/pnas.1212956110,

Chiarello C, Welcome SE, Halderman LK, & Leonard CM (2009). Does degree of asymmetry relate to performance? An investigation of word recognition and reading in consistent and mixed handers. Brain and Cognition, 69, 521–530. 10.1016/j.bandc.2008.11.002, [PubMed: 19100673]

Crow TJ, Done DJ, & Sacker A (1996). Cerebral lateralization is delayed in children who later develop schizophrenia. Schizophrenia Research, 22, 181–185. 10.1016/S0920-9964(96)00068-0, [PubMed: 9000315]

Dale AM, Fischl B, & Sereno MI (1999). Cortical surface-based analysis: I. Segmentation and surface reconstruction. Neuroimage, 9, 179–194. 10.1006/nimg.1998.0395, [PubMed: 9931268]

Desgranges B, Baron J-C, & Eustache F (1998). The functional neuroanatomy of episodic memory: The role of the frontal lobes, the hippocampal formation, and other areas. Neuroimage, 8, 198–213. 10.1006/nimg.1998.0359, [PubMed: 9740762]

DiNicola LM, Braga RM, & Buckner RL (2020). Parallel distributed networks dissociate episodic and social functions within the individual. Journal of Neurophysiology, 123, 1144–1179. 10.1152/jn.00529.2019, [PubMed: 32049593]

DiNicola LM, & Buckner RL (2021). Precision estimates of parallel distributed association networks: Evidence for domain specialization and implications for evolution and development. Current Opinion in Behavioral Sciences, 40, 120–129. 10.1016/j.cobeha.2021.03.029, [PubMed: 34263017]

Doucet G, Naveau M, Petit L, Delcroix N, Zago L, Crivello F, et al. (2011). Brain activity at rest: A multiscale hierarchical functional organization. Journal of Neurophysiology, 105, 2753–2763. 10.1152/jn.00895.2010, [PubMed: 21430278]

Downing PE, Jiang Y, Shuman M, & Kanwisher N (2001). A cortical area selective for visual processing of the human body. Science, 293, 2470–2473. 10.1126/science.1063414, [PubMed: 11577239]

Dundas EM, Plaut DC, & Behrmann M (2015). Variable left-hemisphere language and orthographic lateralization reduces right-hemisphere face lateralization. Journal of Cognitive Neuroscience, 27, 913–925. 10.1162/jocn_a_00757, [PubMed: 25390197]

Dworetsky A, Seitzman BA, Adeyemo B, Neta M, Coalson RS, Petersen SE, et al. (2021). Probabilistic mapping of human functional brain networks identifies regions of high group consensus. Neuroimage, 237, 118164. 10.1016/j.neuroimage.2021.118164, [PubMed: 34000397]

Dworetsky A, Seitzman BA, Adeyemo B, Smith DM, Petersen SE, & Gratton C (2021). Two common and distinct forms of variation in human functional brain networks. bioRxiv. 10.1101/2021.09.17.460799

Dworkin JD, Linn KA, Teich EG, Zurn P, Shinohara RT, & Bassett DS (2020). The extent and drivers of gender imbalance in neuroscience reference lists. Nature Neuroscience, 23, 918–926. 10.1038/s41593-020-0658-y, [PubMed: 32561883]

Escalante-Mead PR, Minshew NJ, & Sweeney JA (2003). Abnormal brain lateralization in high-functioning autism. Journal of Autism and Developmental Disorders, 33, 539–543. 10.1023/A:1025887713788, [PubMed: 14594334]

Esteves M, Lopes SS, Almeida A, Sousa N, & Leite-Almeida H (2020). Unmasking the relevance of hemispheric asymmetries—Break on through (to the other side). Progress in Neurobiology, 192, 101823. 10.1016/j.pneurobio.2020.101823, [PubMed: 32433927]

Everts R, Lidzba K, Wilke M, Kiefer C, Mordasini M, Schroth G, et al. (2009). Strengthening of laterality of verbal and visuospatial functions during childhood and adolescence. Human Brain Mapping, 30, 473–483. 10.1002/hbm.20523, [PubMed: 18219619]

Fair DA, Miranda-Dominguez O, Snyder AZ, Perrone A, Earl EA, Van AN, et al. (2020). Correction of respiratory artifacts in MRI head motion estimates. Neuroimage, 208, 116400. 10.1016/j.neuroimage.2019.116400, [PubMed: 31778819]

Federmeier KD, Wlotko EW, & Meyer AM (2008). What's 'right' in language comprehension: ERPs reveal right hemisphere language capabilities. Language and Linguistics Compass, 2, 1–17. 10.1111/j.1749-818X.2007.00042.x, [PubMed: 19777128]

Fedorenko E, & Blank IA (2020). Broca's area is not a natural kind. Trends in Cognitive Sciences, 24, 270–284. 10.1016/j.tics.2020.01.001, [PubMed: 32160565]

Fedorenko E, Duncan J, & Kanwisher N (2012). Language-selective and domain-general regions lie side by side within Broca's area. Current Biology, 22, 2059–2062. 10.1016/j.cub.2012.09.011, [PubMed: 23063434]

Finn ES, Shen X, Scheinost D, Rosenberg MD, Huang J, Chun MM, et al. (2015). Functional connectome fingerprinting: Identifying individuals using patterns of brain connectivity. Nature Neuroscience, 18, 1664–1671. 10.1038/nn.4135, [PubMed: 26457551]

Floris DL, Wolfers T, Zabihi M, Holz NE, Zwiers MP, Charman T, et al. (2021). Atypical brain asymmetry in autism—A candidate for clinically meaningful stratification. Biological Psychiatry: Cognitive Neuroscience and Neuroimaging, 6, 802–812. 10.1016/j.bpsc.2020.08.008, [PubMed: 33097470]

Friston KJ, Williams S, Howard R, Frackowiak RSJ, & Turner R (1996). Movement-related effects in fMRI time-series: Movement artifacts in fMRI. Magnetic Resonance in Medicine, 35, 346–355. 10.1002/mrm.1910350312, [PubMed: 8699946]

Fukuchi-Shimogori T, & Grove EA (2001). Neocortex patterning by the secreted signaling molecule FGF8. Science, 294, 1071–1074. 10.1126/science.1064252, [PubMed: 11567107]

Fulvio JM, Akinnola I, & Postle BR (2021). Gender (im)balance in citation practices in cognitive neuroscience. Journal of Cognitive Neuroscience, 33, 3–7. 10.1162/jocn_a_01643, [PubMed: 33078992]

Garel S, Huffman KJ, & Rubenstein JLR (2003). Molecular regionalization of the neocortex is disrupted in *Fgf8* hypomorphic mutants. Development, 130, 1903–1914. 10.1242/dev.00416, [PubMed: 12642494]

Geschwind N, & Levitsky W (1968). Human brain: Left–right asymmetries in temporal speech region. Science, 161, 186–187. 10.1126/science.161.3837.186, [PubMed: 5657070]

Glasser MF, Smith SM, Marcus DS, Andersson JLR, Auerbach EJ, Behrens TEJ, et al. (2016). The Human Connectome Project's neuroimaging approach. Nature Neuroscience, 19, 1175–1187. 10.1038/nn.4361, [PubMed: 27571196]

Glasser MF, Sotiropoulos SN, Wilson JA, Coalson TS, Fischl B, Andersson JL, et al. (2013). The minimal preprocessing pipelines for the Human Connectome Project. Neuroimage, 80, 105–124. 10.1016/j.neuroimage.2013.04.127, [PubMed: 23668970]

Glasser MF, & Van Essen DC (2011). Mapping human cortical areas in vivo based on myelin content as revealed by T1- and T2-weighted MRI. Journal of Neuroscience, 31, 11597–11616. 10.1523/JNEUROSCI.2180-11.2011, [PubMed: 21832190]

Gordon EM, Laumann TO, Adeyemo B, Huckins JF, Kelley WM, & Petersen SE (2016). Generation and evaluation of a cortical area Parcellation from resting-state correlations. Cerebral Cortex, 26, 288–303. 10.1093/cercor/bhu239, [PubMed: 25316338]

Gordon EM, Laumann TO, Adeyemo B, & Petersen SE (2017). Individual variability of the system-level organization of the human brain. Cerebral Cortex, 27, 386–399. 10.1093/cercor/bhv239, [PubMed: 26464473]

Gordon EM, Laumann TO, Gilmore AW, Newbold DJ, Greene DJ, Berg JJ, et al. (2017). Precision functional mapping of individual human brains. Neuron, 95, 791–807. 10.1016/j.neuron.2017.07.011, [PubMed: 28757305]

Gotts SJ, Jo HJ, Wallace GL, Saad ZS, Cox RW, & Martin A (2013). Two distinct forms of functional lateralization in the human brain. Proceedings of the National Academy of Sciences, U.S.A, 110, E3435–E3444. 10.1073/pnas.1302581110,

Gratton C, Dworetsky A, Coalson RS, Adeyemo B, Laumann TO, Wig GS, et al. (2020). Removal of high frequency contamination from motion estimates in single-band fMRI saves data without

biasing functional connectivity. Neuroimage, 217, 116866. 10.1016/j.neuroimage.2020.116866, [PubMed: 32325210]

Gratton C, Neta M, Sun H, Ploran EJ, Schlaggar BL, Wheeler ME, et al. (2017). Distinct stages of moment-to-moment processing in the cingulo-opercular and frontoparietal networks. Cerebral Cortex, 27, 2403–2417. 10.1093/cercor/bhw092, [PubMed: 27095824]

Greene DJ, Marek S, Gordon EM, Siegel JS, Gratton C, Laumann TO, et al. (2020). Integrative and network-specific connectivity of the basal ganglia and thalamus defined in individuals. Neuron, 105, 742–758. 10.1016/j.neuron.2019.11.012, [PubMed: 31836321]

Güntürkün O, Diekamp B, Manns M, Nottelmann F, Prior H, Schwarz A, et al. (2000). Asymmetry pays: Visual lateralization improves discrimination success in pigeons. Current Biology, 10, 1079–1081. 10.1016/S0960-9822(00)00671-0, [PubMed: 10996079]

Güntürkün O, & Ocklenburg S (2017). Ontogenesis of lateralization. Neuron, 94, 249–263. 10.1016/j.neuron.2017.02.045, [PubMed: 28426959]

Hill J, Inder T, Neil J, Dierker D, Harwell J, & Van Essen D (2010). Similar patterns of cortical expansion during human development and evolution. Proceedings of the National Academy of Sciences, U.S.A, 107, 13135–13140. 10.1073/pnas.1001229107,

Hou L, Xiang L, Crow TJ, Leroy F, Rivière D, Mangin J-F, et al. (2019). Measurement of Sylvian Fissure asymmetry and occipital bending in humans and Pan troglodytes. Neuroimage, 184, 855–870. 10.1016/j.neuroimage.2018.08.045, [PubMed: 30170149]

Hunt DL, Yamoah EN, & Krubitzer LA (2006). Multisensory plasticity in congenitally deaf mice: How are cortical areas functionally specified? Neuroscience, 139, 1507–1524. 10.1016/j.neuroscience.2006.01.023, [PubMed: 16529873]

Huntenburg JM, Bazin P-L, & Margulies DS (2018). Large-scale gradients in human cortical organization. Trends in Cognitive Sciences, 22, 21–31. 10.1016/j.tics.2017.11.002, [PubMed: 29203085]

Hutsler J, & Galuske RAW (2003). Hemispheric asymmetries in cerebral cortical networks. Trends in Neurosciences, 26, 429–435. 10.1016/S0166-2236(03)00198-X, [PubMed: 12900174]

Jouravlev O, Kell AJE, Mineroff Z, Haskins AJ, Ayyash D, Kanwisher N, et al. (2020). Reduced language lateralization in autism and the broader autism phenotype as assessed with robust individual-subjects analyses. Autism Research, 13, 1746–1761. 10.1002/aur.2393, [PubMed: 32935455]

Jung-Beeman M (2005). Bilateral brain processes for comprehending natural language. Trends in Cognitive Sciences, 9, 512–518. 10.1016/j.tics.2005.09.009, [PubMed: 16214387]

Kahn DM, & Krubitzer L (2002). Massive cross-modal cortical plasticity and the emergence of a new cortical area in developmentally blind mammals. Proceedings of the National Academy of Sciences, U.S.A, 99, 11429–11434. 10.1073/pnas.162342799,

Kanwisher N, McDermott J, & Chun MM (1997). The fusiform face area: A module in human extrastriate cortex specialized for face perception. Journal of Neuroscience, 17, 4302–4311. 10.1523/JNEUROSCI.17-11-04302.1997, [PubMed: 9151747]

Knecht S, Dräger B, Deppe M, Bobe L, Lohmann H, Flöel A, et al. (2000). Handedness and hemispheric language dominance in healthy humans. Brain, 123, 2512–2518. 10.1093/brain/123.12.2512, [PubMed: 11099452]

Kong R, Li J, Orban C, Sabuncu MR, Liu H, Schaefer A, et al. (2019). Spatial topography of individual-specific cortical networks predicts human cognition, personality, and emotion. Cerebral Cortex, 29, 2533–2551. 10.1093/cercor/bhy123, [PubMed: 29878084]

Kong X-Z, Mathias SR, Guadalupe T, ENIGMA Laterality Working Group, Glahn DC, Franke B, et al. (2018). Mapping cortical brain asymmetry in 17,141 healthy individuals worldwide via the ENIGMA Consortium. Proceedings of the National Academy of Sciences, U.S.A, 115, E5154–E5163. 10.1073/pnas.1718418115,

Kong X-Z, Postema M, Schijven D, Carrión Castillo A, Pepe A, Crivello F, et al. (2021). Large-scale phenomic and genomic analysis of brain asymmetrical skew. Cerebral Cortex, 31, 4151–4168. 10.1093/cercor/bhab075, [PubMed: 33836062]

Kraus BT, Perez D, Ladwig Z, Seitzman BA, Dworetsky A, Petersen SE, et al. (2021). Network variants are similar between task and rest states. Neuroimage, 229, 117743. 10.1016/j.neuroimage.2021.117743, [PubMed: 33454409]

Krubitzer L (2007). The magnificent compromise: Cortical field evolution in mammals. Neuron, 56, 201–208. 10.1016/j.neuron.2007.10.002, [PubMed: 17964240]

Krubitzer LA, & Seelke AMH (2012). Cortical evolution in mammals: The bane and beauty of phenotypic variability. Proceedings of the National Academy of Sciences, U.S.A, 109(Suppl. 1), 10647–10654. 10.1073/pnas.1201891109,

Lake EMR, Finn ES, Noble SM, Vanderwal T, Shen X, Rosenberg MD, et al. (2019). The functional brain organization of an individual allows prediction of measures of social abilities transdiagnostically in autism and attention-deficit/hyperactivity disorder. Biological Psychiatry, 86, 315–326. 10.1016/j.biopsych.2019.02.019, [PubMed: 31010580]

Laumann TO, Gordon EM, Adeyemo B, Snyder AZ, Joo SJ, Chen M-Y, et al. (2015). Functional system and areal organization of a highly sampled individual human brain. Neuron, 87, 657–670. 10.1016/j.neuron.2015.06.037, [PubMed: 26212711]

Levy J (1977). The mammalian brain and the adaptive advantage of cerebral asymmetry. Annals of the New York Academy of Sciences, 299, 264–272. 10.1111/j.1749-6632.1977.tb41913.x, [PubMed: 280207]

Li S-C, & Lindenberger U (1999). Cross-level unification: A computational exploration of the link between deterioration of neurotransmitter systems and dedifferentiation of cognitive abilities in old age. In Cognitive science of memory (pp. 103–146). Hogrefe & Huber.

Lidzba K, Schwilling E, Grodd W, Krägeloh-Mann I, & Wilke M (2011). Language comprehension vs. language production: Age effects on fMRI activation. Brain and Language, 119, 6–15. 10.1016/j.bandl.2011.02.003, [PubMed: 21450336]

Lindell AK (2006). In your right mind: Right hemisphere contributions to language processing and production. Neuropsychology Review, 16, 131–148. 10.1007/s11065-006-9011-9, [PubMed: 17109238]

Lindell AK, & Hudry K (2013). Atypicalities in cortical structure, handedness, and functional lateralization for language in autism spectrum disorders. Neuropsychology Review, 23, 257–270. 10.1007/s11065-013-9234-5, [PubMed: 23649809]

Lipkin B, Tuckute G, Affourtit J, Small H, Mineroff Z, Kean H, et al. (2022). Probabilistic atlas for the language network based on precision fMRI data from >800 individuals. Scientific Data, 9, 529. 10.1038/s41597-022-01645-3, [PubMed: 36038572]

Liu J, Tsang T, Jackson L, Ponting C, Jeste SS, Bookheimer SY, et al. (2019). Altered lateralization of dorsal language tracts in 6-week-old infants at risk for autism. Developmental Science, 22, e12768. 10.1111/desc.12768, [PubMed: 30372577]

Marek S, & Dosenbach NUF (2018). The frontoparietal network: Function, electrophysiology, and importance of individual precision mapping. Dialogues in Clinical Neuroscience, 20, 133–140. 10.31887/DCNS.2018.20.2/smarek, [PubMed: 30250390]

Mars RB, Neubert F-X, Noonan MP, Sallet J, Toni I, & Rushworth MFS (2012). On the relationship between the “default mode network” and the “social brain.” Frontiers in Human Neuroscience, 6, 189. 10.3389/fnhum.2012.00189, [PubMed: 22737119]

Mesulam M-M (1998). From sensation to cognition. Brain, 121, 1013–1052. 10.1093/brain/121.6.1013, [PubMed: 9648540]

Miranda-Dominguez O, Mills BD, Carpenter SD, Grant KA, Kroenke CD, Nigg JT, et al. (2014). Connectotyping: Model based fingerprinting of the functional connectome. PLoS One, 9, e111048. 10.1371/journal.pone.0111048, [PubMed: 25386919]

Mueller S, Wang D, Fox MD, Yeo BTT, Sepulcre J, Sabuncu MR, et al. (2013). Individual variability in functional connectivity architecture of the human brain. Neuron, 77, 586–595. 10.1016/j.neuron.2012.12.028, [PubMed: 23395382]

Newbold DJ, Gordon EM, Laumann TO, Seider NA, Montez DF, Gross SJ, et al. (2021). Cingulo-opercular control network and disused motor circuits joined in standby mode. Proceedings of the National Academy of Sciences, U.S.A, 118, e2019128118. 10.1073/pnas.2019128118,

Nielsen JA, Zielinski BA, Fletcher PT, Alexander AL, Lange N, Bigler ED, et al. (2014). Abnormal lateralization of functional connectivity between language and default mode regions in autism. Molecular Autism, 5, 8. 10.1186/2040-2392-5-8, [PubMed: 24502324]

Oertel-Knöchel V, & Linden DEJ (2011). Cerebral asymmetry in schizophrenia. Neuroscientist, 17, 456–467. 10.1177/1073858410386493, [PubMed: 21518811]

Oldfield RC (1971). The assessment and analysis of handedness: The Edinburgh inventory. Neuropsychologia, 9, 97–113. 10.1016/0028-3932(71)90067-4, [PubMed: 5146491]

O'Leary DDM, Chou S-J, & Sahara S (2007). Area patterning of the mammalian cortex. Neuron, 56, 252–269. 10.1016/j.neuron.2007.10.010, [PubMed: 17964244]

Perlaki G, Horvath R, Orsi G, Aradi M, Auer T, Varga E, et al. (2013). White-matter microstructure and language lateralization in left-handers: A whole-brain MRI analysis. Brain and Cognition, 82, 319–328. 10.1016/j.bandc.2013.05.005, [PubMed: 23792788]

Power JD, Barnes KA, Snyder AZ, Schlaggar BL, & Petersen SE (2012). Spurious but systematic correlations in functional connectivity MRI networks arise from subject motion. Neuroimage, 59, 2142–2154. 10.1016/j.neuroimage.2011.10.018, [PubMed: 22019881]

Power JD, Cohen AL, Nelson SM, Wig GS, Barnes KA, Church JA, et al. (2011). Functional network organization of the human brain. Neuron, 72, 665–678. 10.1016/j.neuron.2011.09.006, [PubMed: 22099467]

Power JD, Mitra A, Laumann TO, Snyder AZ, Schlaggar BL, & Petersen SE (2014). Methods to detect, characterize, and remove motion artifact in resting state fMRI. Neuroimage, 84, 320–341. 10.1016/j.neuroimage.2013.08.048, [PubMed: 23994314]

Power JD, Schlaggar BL, Lessov-Schlaggar CN, & Petersen SE (2013). Evidence for hubs in human functional brain networks. Neuron, 79, 798–813. 10.1016/j.neuron.2013.07.035, [PubMed: 23972601]

Power JD, Schlaggar BL, & Petersen SE (2015). Recent progress and outstanding issues in motion correction in resting state fMRI. Neuroimage, 105, 536–551. 10.1016/j.neuroimage.2014.10.044, [PubMed: 25462692]

Reuter-Lorenz PA, & Cappell KA (2008). Neurocognitive aging and the compensation hypothesis. Current Directions in Psychological Science, 17, 177–182. 10.1111/j.1467-8721.2008.00570.x

Rogers LJ, Zucca P, & Vallortigara G (2004). Advantages of having a lateralized brain. Proceedings of the Royal Society of London, Series B: Biological Sciences, 271(Suppl. 6), S420–S422. 10.1098/rsbl.2004.0200,

Rugg MD, & Vilberg KL (2013). Brain networks underlying episodic memory retrieval. Current Opinion in Neurobiology, 23, 255–260. 10.1016/j.conb.2012.11.005, [PubMed: 23206590]

Saxe R, & Kanwisher N (2003). People thinking about thinking people: The role of the temporo-parietal junction in "theory of mind." Neuroimage, 19, 1835–1842. 10.1016/S1053-8119(03)00230-1, [PubMed: 12948738]

Schwarzkopf DS, Song C, & Rees G (2011). The surface area of human V1 predicts the subjective experience of object size. Nature Neuroscience, 14, 28–30. 10.1038/nn.2706, [PubMed: 21131954]

Seitzman BA, Gratton C, Laumann TO, Gordon EM, Adeyemo B, Dworetsky A, et al. (2019). Trait-like variants in human functional brain networks. Proceedings of the National Academy of Sciences, U.S.A, 116, 22851–22861. 10.1073/pnas.1902932116,

Sen S, Khalsa NN, Tong N, Ovadia-Caro S, Wang X, Bi Y, et al. (2022). The role of visual experience in individual differences of brain connectivity. Journal of Neuroscience, 42, 5070–5084. 10.1523/JNEUROSCI.1700-21.2022, [PubMed: 35589393]

Shen X, Finn ES, Scheinost D, Rosenberg MD, Chun MM, Papademetris X, et al. (2017). Using connectome-based predictive modeling to predict individual behavior from brain connectivity. Nature Protocols, 12, 506–518. 10.1038/nprot.2016.178, [PubMed: 28182017]

Smith SM, Fox PT, Miller KL, Glahn DC, Fox PM, Mackay CE, et al. (2009). Correspondence of the brain's functional architecture during activation and rest. Proceedings of the National Academy of Sciences, U.S.A, 106, 13040–13045. 10.1073/pnas.0905267106,

Sommer I, Aleman A, Ramsey N, Bouma A, & Kahn R (2001). Handedness, language lateralisation and anatomical asymmetry in schizophrenia: Meta-analysis. British Journal of Psychiatry, 178, 344–351. 10.1192/bjp.178.4.344,

Sood G, & Laohaprapanon S (2018). Predicting race and ethnicity from the sequence of characters in a name. arXiv:1805.02109. 10.48550/arXiv.1805.02109

Spreng RN, Sepulcre J, Turner GR, Stevens WD, & Schacter DL (2013). Intrinsic architecture underlying the relations among the default, dorsal attention, and frontoparietal control networks of the human brain. Journal of Cognitive Neuroscience, 25, 74–86. 10.1162/jocn_a_00281, [PubMed: 22905821]

Spreng RN, Stevens WD, Chamberlain JP, Gilmore AW, & Schacter DL (2010). Default network activity, coupled with the frontoparietal control network, supports goal-directed cognition. Neuroimage, 53, 303–317. 10.1016/j.neuroimage.2010.06.016, [PubMed: 20600998]

Srihasam K, Vincent JL, & Livingstone MS (2014). Novel domain formation reveals proto-architecture in inferotemporal cortex. Nature Neuroscience, 17, 1776–1783. 10.1038/nn.3855, [PubMed: 25362472]

Steinmetz H (1996). Structure, function and cerebral asymmetry: In vivo morphometry of the planum temporale. Neuroscience & Biobehavioral Reviews, 20, 587–591. 10.1016/0149-7634(95)00071-2, [PubMed: 8994197]

Stippich C, Mohammed J, Kress B, Hähnel S, Günther J, Konrad F, et al. (2003). Robust localization and lateralization of human language function: An optimized clinical functional magnetic resonance imaging protocol. Neuroscience Letters, 346, 109–113. 10.1016/S0304-3940(03)00561-5, [PubMed: 12850560]

Striem-Amit E, Ovadia-Caro S, Caramazza A, Margulies DS, Villringer A, & Amedi A (2015). Functional connectivity of visual cortex in the blind follows retinotopic organization principles. Brain, 138, 1679–1695. 10.1093/brain/awv083, [PubMed: 25869851]

Sur M, & Rubenstein JLR (2005). Patterning and plasticity of the cerebral cortex. Science, 310, 805–810. 10.1126/science.1112070, [PubMed: 16272112]

Szaflarski JP, Holland SK, Schmithorst VJ, & Byars AW (2006). fMRI study of language lateralization in children and adults. Human Brain Mapping, 27, 202–212. 10.1002/hbm.20177, [PubMed: 16035047]

Tavor I, Jones OP, Mars RB, Smith SM, Behrens TE, & Jbabdi S (2016). Task-free MRI predicts individual differences in brain activity during task performance. Science, 352, 216–220. 10.1126/science.aad8127, [PubMed: 27124457]

Toga AW, & Thompson PM (2003). Mapping brain asymmetry. Nature Reviews Neuroscience, 4, 37–48. 10.1038/nrn1009, [PubMed: 12511860]

Tulving E, Kapur S, Craik FI, Moscovitch M, & Houle S (1994). Hemispheric encoding/retrieval asymmetry in episodic memory: Positron emission tomography findings. Proceedings of the National Academy of Sciences, U.S.A, 91, 2016–2020. 10.1073/pnas.91.6.2016,

Van Essen DC, Glasser MF, Dierker DL, Harwell J, & Coalson T (2012). Parcellations and hemispheric asymmetries of human cerebral cortex analyzed on surface-based atlases. Cerebral Cortex, 22, 2241–2262. 10.1093/cercor/bhr291, [PubMed: 22047963]

Van Essen DC, Smith SM, Barch DM, Behrens TEJ, Yacoub E, & Ugurbil K (2013). The WU-Minn Human Connectome Project: An overview. Neuroimage, 80, 62–79. 10.1016/j.neuroimage.2013.05.041, [PubMed: 23684880]

Van Essen DC, Ugurbil K, Auerbach E, Barch D, Behrens TEJ, Bucholz R, et al. (2012). The Human Connectome Project: A data acquisition perspective. Neuroimage, 62, 2222–2231. 10.1016/j.neuroimage.2012.02.018, [PubMed: 22366334]

Verghese A, Kolbe SC, Anderson AJ, Egan GF, & Vidyasagar TR (2014). Functional size of human visual area V1: A neural correlate of top–down attention. Neuroimage, 93, 47–52. 10.1016/j.neuroimage.2014.02.023, [PubMed: 24583254]

Wang D, Buckner RL, & Liu H (2014). Functional specialization in the human brain estimated by intrinsic hemispheric interaction. Journal of Neuroscience, 34, 12341–12352. 10.1523/JNEUROSCI.0787-14.2014, [PubMed: 25209275]

Weintraub S, & Mesulam M-M (1987). Right cerebral dominance in spatial attention: Further evidence based on ipsilateral neglect. Archives of Neurology, 44, 621–625. 10.1001/archneur.1987.00520180043014, [PubMed: 3579679]

Yeo BTT, Krienen FM, Sepulcre J, Sabuncu MR, Lashkari D, Hollinshead M, et al. (2011). The organization of the human cerebral cortex estimated by intrinsic functional connectivity. Journal of Neurophysiology, 106, 1125–1165. 10.1152/jn.00338.2011, [PubMed: 21653723]

Zhou D, Cornblath EJ, Stiso J, Teich EG, Dworkin JD, Blevins AS, et al. (2020). Gender diversity statement and code notebook v1.0. Zenodo. 10.5281/zenodo.3672110

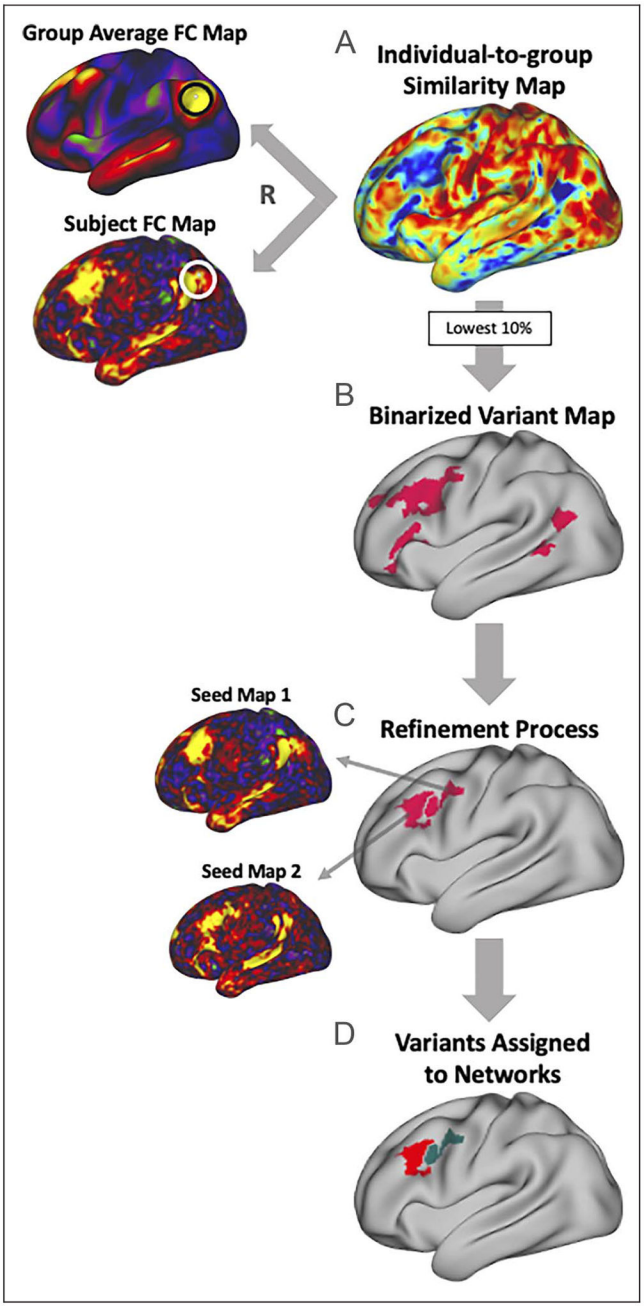

Figure 1.

Procedure for identifying "network variants," locations of strong individual differences in functional brain networks. Network variant regions are identified by comparing the functional connectivity of an individual to that of a group average derived from data from 120 young adults (WashU 120; see Methods). (A) First, a vertex-wise comparison of an individual-specific functional connectivity map and the group average (shown for a seed located near TPJ) is calculated using spatial correlation, resulting in an individual-to-group similarity map containing a continuous similarity value at each vertex. (B) The individual-to-group similarity map is then binarized to the lowest 10% of correlations to identify

regions where the individual is most different from the group; small regions or regions with low BOLD signal are excluded. (C) These initial contiguous regions are then split into separable homogenous clusters as in Dworetsky, Seitzman, Adeyemo, Smith, et al. (2021) (see Methods), and small clusters (<30 vertices) were removed. Shown are average seed maps for two separable clusters that were split during the refinement process. (D) Lastly, each resulting variant region is assigned to the canonical network to which its average seed map is most similar, judged via Dice coefficient.

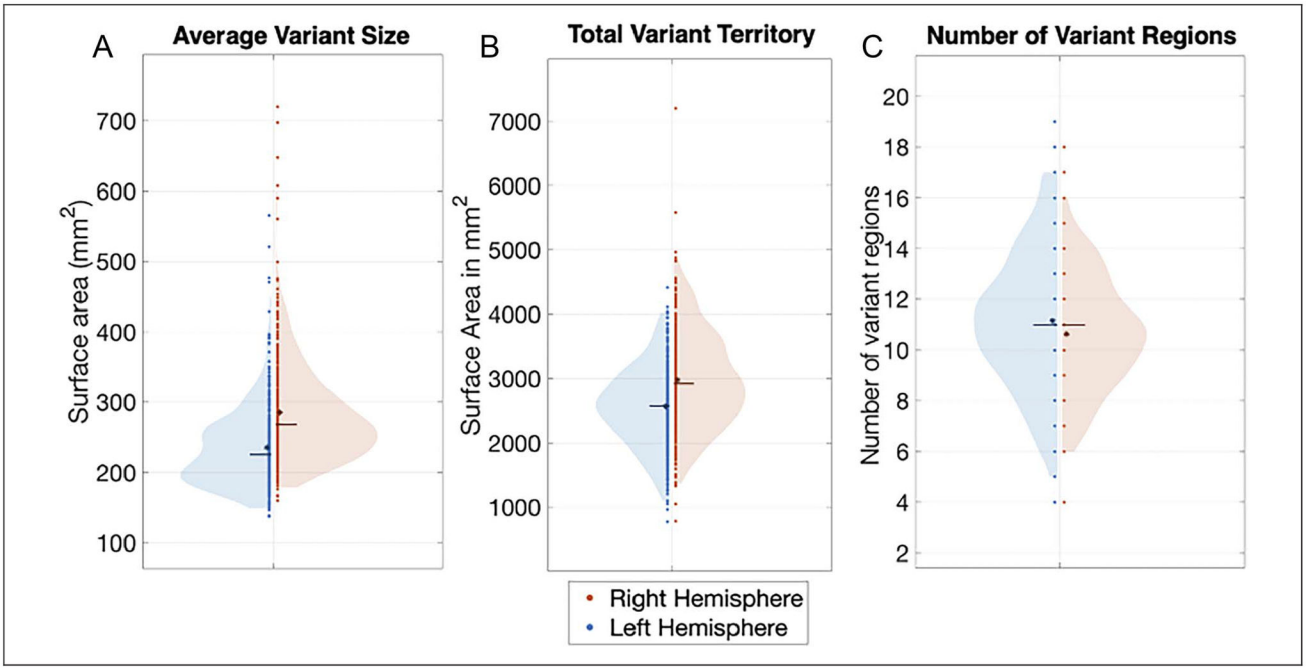

Figure 2.

Comparison of the average number of separable variant regions and variant vertices, and average variant size across hemispheres. The violin plots show the distribution of measures of (A) average variant size in surface area (in mm^2), (B) average total variant territory, and (C) average number of network variant regions in the left hemisphere (left side of violin plot, blue) and the right hemisphere (right side of violin plot, red). An asterisk indicates the mean, and a line indicates the median of each distribution. Network variants in the right hemisphere were larger and covered significantly more surface area than in the left hemisphere. Left-hemisphere variants were slightly more numerous (but this effect was somewhat more dependent on processing choices).

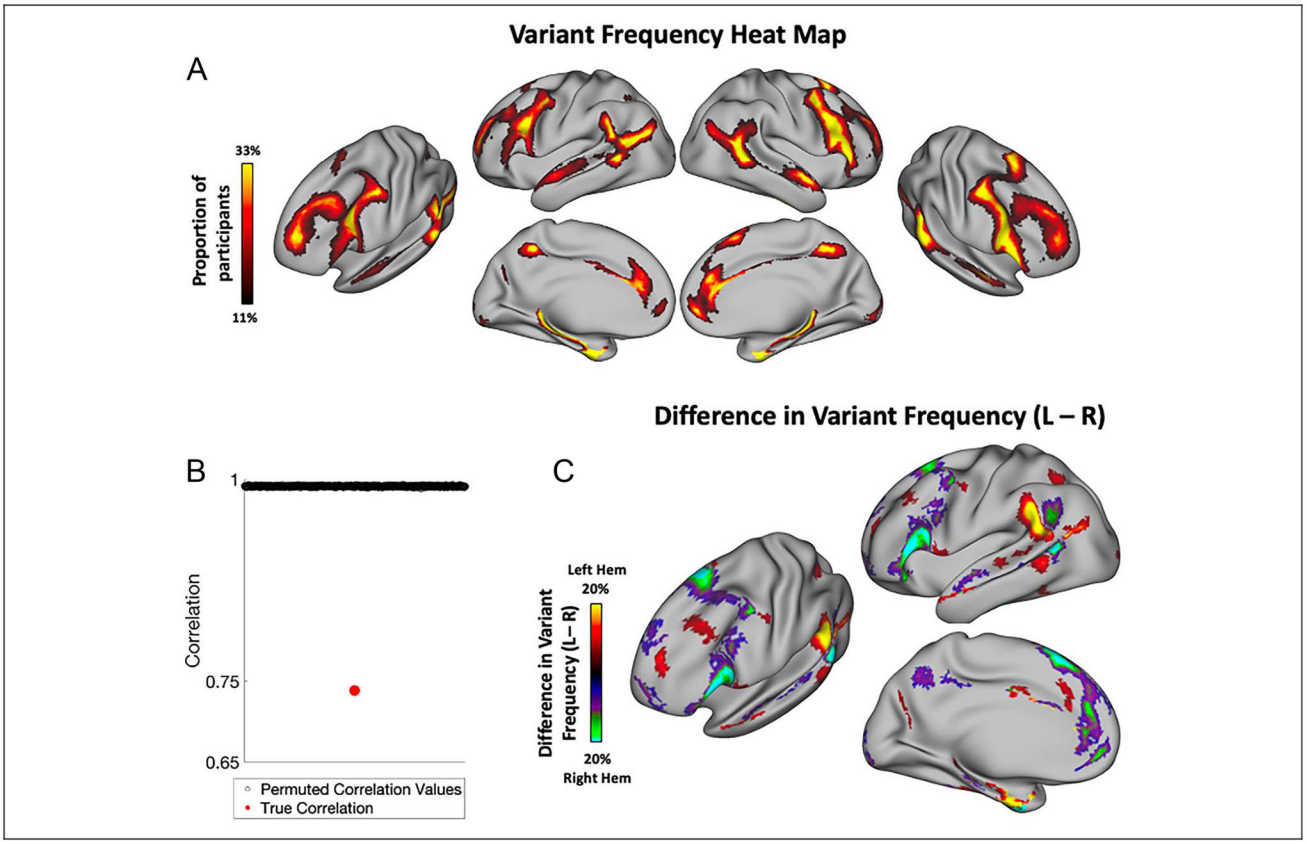

Figure 3.

Hemispheric asymmetries in the spatial distribution of network variants. (A) Frequency of network variants across 384 unrelated participants from the HCP. Network variants have a high frequency in regions of association cortex. (B) Permutation test examining the correlation between variant overlap maps of left and right hemispheres. Permuted correlation values indicate correlations between overlap maps obtained by randomly flipping the left and right hemispheres of participants (see Methods); red dot indicates the true correlation. The two hemispheres have significantly lower similarity than expected by chance. (C) A difference map (projected on the left hemisphere for visualization) shows the regions in which the two hemispheres differ in the proportion of variant frequency, $p < .05$ cluster-corrected at a frequency difference threshold of 5% (see Appendix C for other thresholds). Warm colors indicate a higher proportion of participants that have a variant at that vertex in left hemisphere, whereas cool colors indicate a higher proportion of participants that have a variant at that vertex in right hemisphere. The spatial distribution of network variants differs significantly across the two hemispheres, with the biggest differences observed in the inferior frontal gyrus, near the temporal parietal junction, and other localized areas of the frontal cortex.

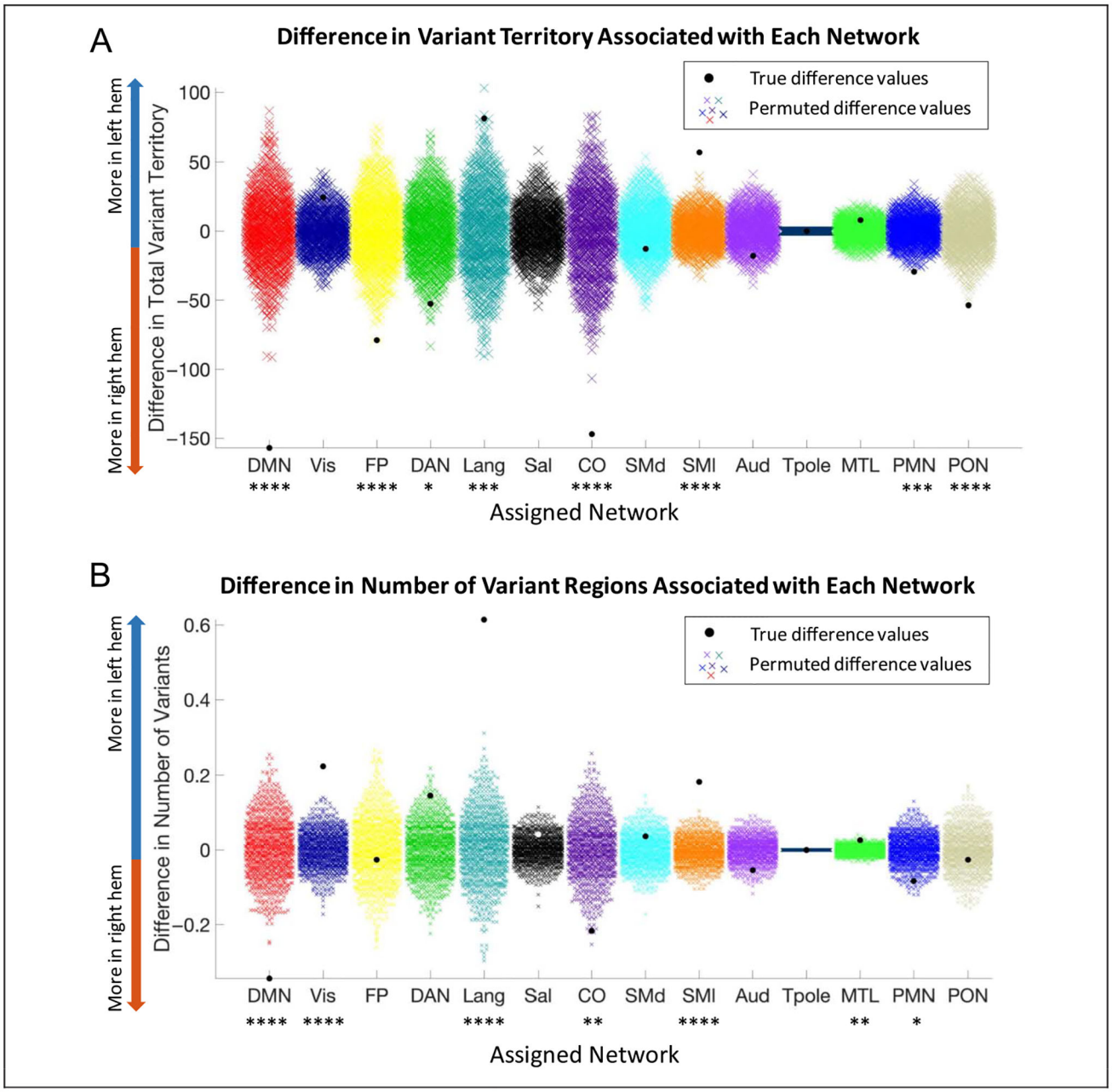

Figure 4.

Hemispheric differences in network assignment of variants. A comparison of the (A) total variant territory and (B) number of variant regions associated with each network in the left and right hemispheres (color = network). Permutation testing shows that the language and somatomotor lateral have increased variant territory in the left hemisphere, whereas the default mode, frontoparietal, dorsal attention, cingulo-opercular, parietal memory, and parietal occipital networks have more variant territory in the right hemisphere. Similarly, the visual, language, somatomotor lateral, and MTL networks have significantly more variant regions in the left hemisphere, whereas the default mode, cingulo-opercular, and parietal

memory networks have significantly more variants in the right hemisphere than would be expected by chance. ****$p < .001$, ***$p < .004$, **$p < .01$, *$p < .02$.

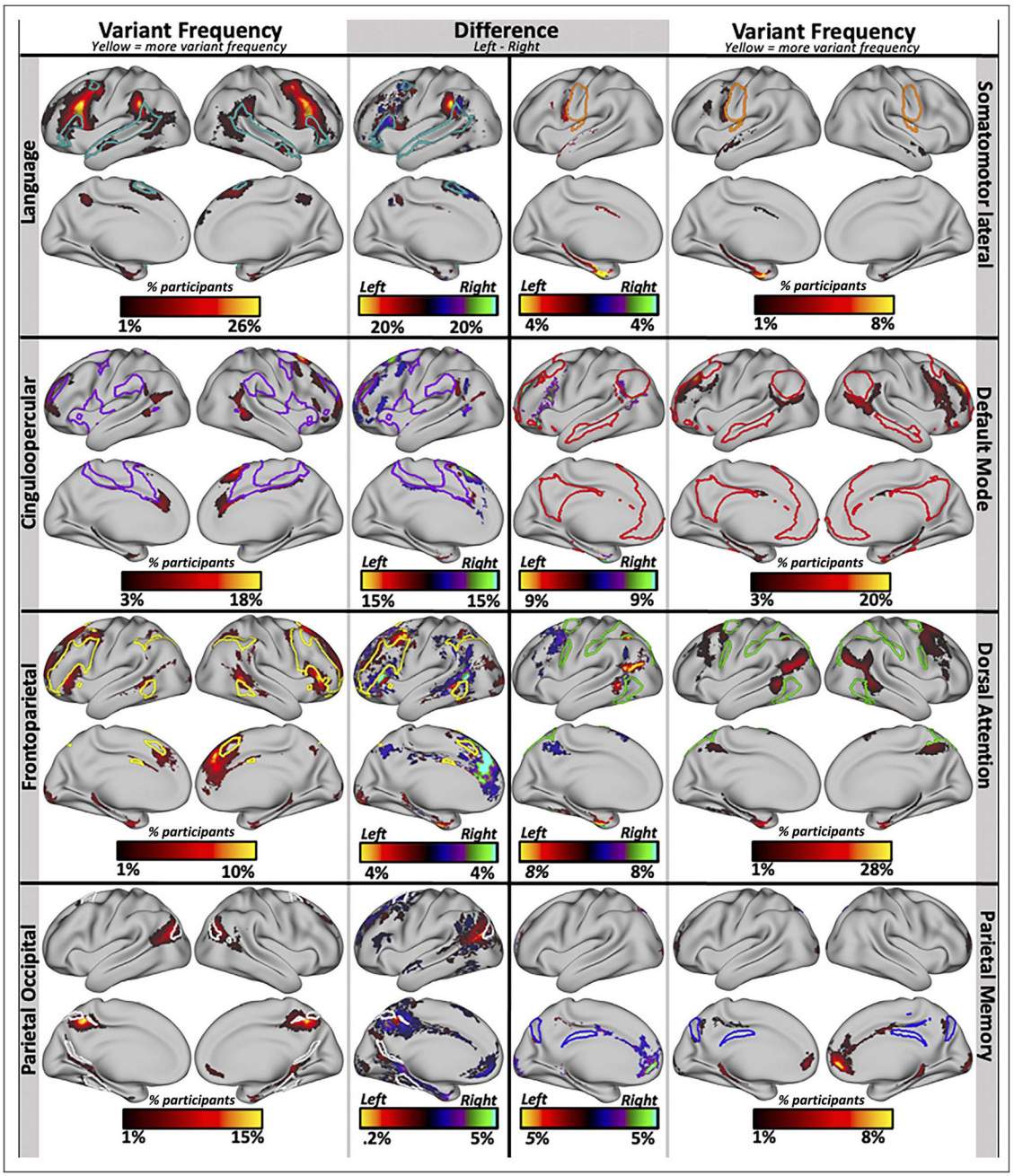

Figure 5.

Areas of asymmetry in networks that showed significant hemispheric differences in their number of network variants. We examined the networks that showed significant hemispheric asymmetries in variant frequency in more depth to observe the regions where they differ the most across the two hemispheres. The language and somatomotor lateral networks have overall higher frequency of variant territory in the left hemisphere, whereas the cingulo-opercular, default mode, frontoparietal, dorsal attention, parietal occipital, and parietal memory networks have higher frequency of variant territory in the right hemisphere. The lateral segments show variant frequency maps, where the color reflects the proportion of

participants that have a variant for each network at that location. Note that the scale is different for each network to maximize visibility. The medial columns show difference maps where the right-hemisphere frequency map was subtracted from the left-hemisphere frequency map to show regions where the two hemispheres differ the most. Warm colors reflect higher variant frequency in the left hemisphere, and cool colors indicate higher variant frequency in the right hemisphere. In each map, the colored outlines show the borders of the canonical network. Variant frequency and difference maps have not been cluster corrected and are presented primarily for qualitative comparisons.

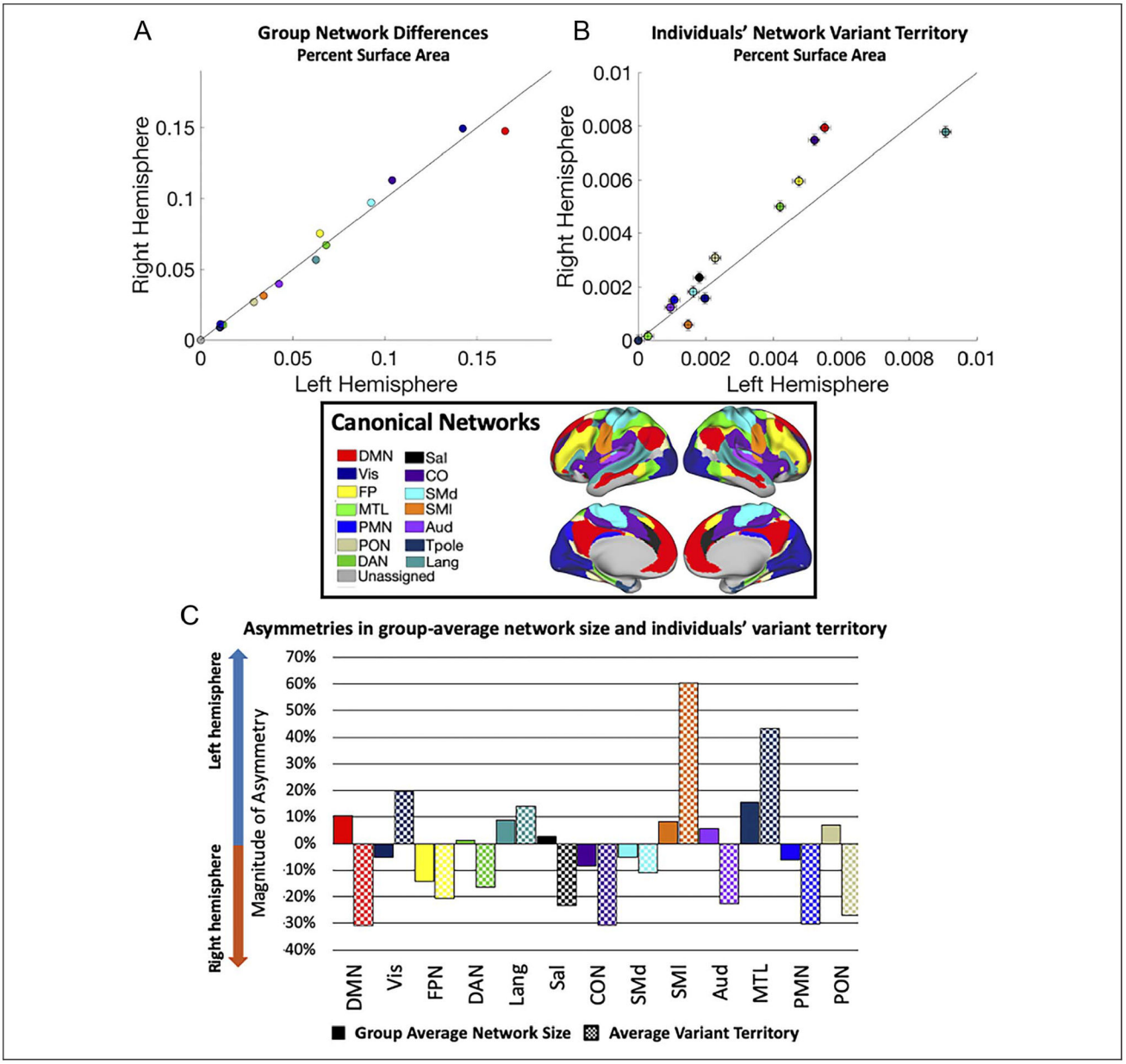

Figure 6.

Asymmetries in group-average network size and number of variants. (A) A comparison of group-average network surface areas in left (*x* axis) and right (*y* axis) hemispheres (color = network, area expressed as a percent of total surface area). These group-average networks are largely symmetrical, with some small-scale differences. (B) Network variant territory associated with specific networks for the left (*x*-axis) and right (*y*-axis) hemispheres (error bars = *SEM*). (C) The magnitude of hemispheric asymmetries in size of group-average networks and variant surface area per network were quantified. The variant territory differs across the two hemispheres, sometimes in the same and sometimes in opposing directions from the asymmetries seen in the group-average maps.

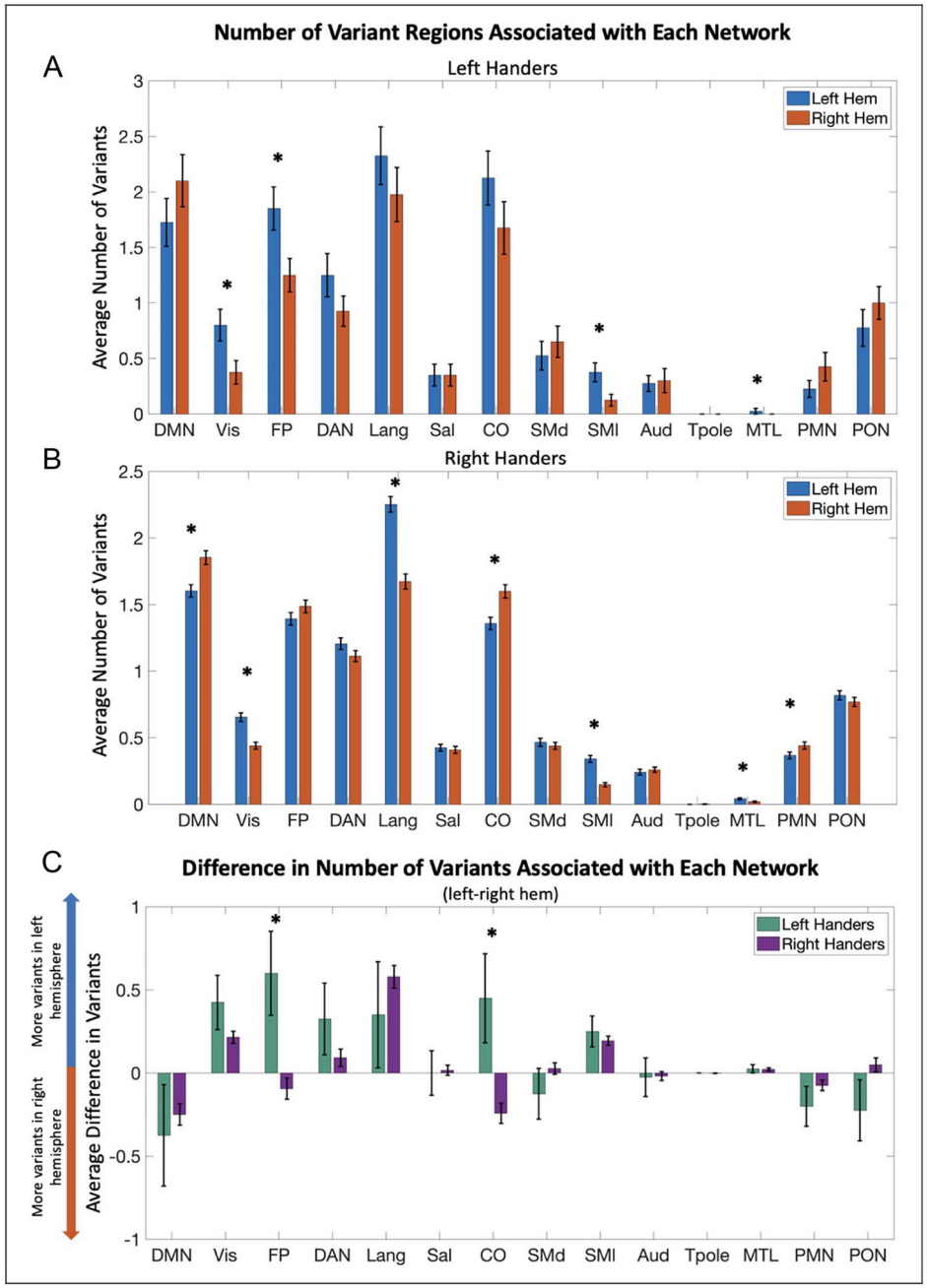

Figure 7.

Difference in network assignment of variants across handedness groups. Comparison in the number of variants associated with each network across left and right hemispheres in (A) left-handers and (B) right-handers. Left-handed individuals showed significant differences in visual, frontoparietal, somatomotor lateral, and medial-temporal lobe networks, with more variants in the left hemisphere. Right-handed participants have significantly more right hemisphere variants associated with default mode, cingulo-opercular, and parietal memory networks and more left-hemisphere variants linked to visual, language, somatomotor lateral, and medial-temporal lobe networks. (C) The bar graph shows the average difference across

participants in the number of variants associated with each functional network in their left minus their right hemisphere. Interactions between handedness and hemisphere were found for frontoparietal ($p = .006$) and cingulo-opercular ($p = .002$) network variants. These comparisons remained significant after FDR correction across all network comparisons. Error bars indicate *SEM*.